Building Drift Estimation Using Acceleration and Strain Measurements

By

Abdulaziz Almarshad
B.S., Qassim University, 2012

Submitted to the graduate degree program in Civil Engineering and the Graduate Faculty of The University of Kansas in partial fulfillment of the requirements for the degree of Master of Science in Civil Engineering.

_____

Chairperson: Prof. Jian Li

_____

Co-Chair: Prof. Andrés Lepage

_____

Prof. Rémy Lequesne

Date Defended: March 17, 2017

The Thesis Committee for Abdulaziz Almarshad certifies that this is the approved version of the following thesis:

Building Drift Estimation Using Acceleration and Strain Measurements

_____

Chair: Prof. Jian Li

_____

Co-Chair: Prof. Andrés Lepage

Date Approved: March 17, 2017

Abstract

Estimating structural displacements is an essential tool in structural engineering. Different methods have been developed to estimate structural displacements either using direct or indirect measurements. One of the common indirect measurements widely used is the acceleration measurement, due to its lower cost and simple instrument attachment to the structures, and it does not require a fixed reference point as most of direct measurements do. This study presents three methods to estimate structural displacement using acceleration and strain measurements. The first method is based on modifying the time-domain finite impulse response (FIR) filter method to estimate displacements using acceleration measurements through a moving time window. This method is verified using measured data from shake table tests on a small-scale structure. The second method converts strain measurements into displacements based on a scaling strategy, in which acceleration measurements and an assumed diagonal mass matrix are used to derive the modal participation mass ratios. The third method, which is the data fusion method, combines the first two. The use and outcome of all three methods are illustrated with numerical results.

Acknowledgements

First, I would like to thank my advisor Prof. Jian Li from the bottom of my heart for his support and advice during completing this thesis work. His guidance and enormous support was a key in completing my degree. Dr. Li offers me his support and time to guide me to correct knowledge and to correct my mistakes. I have been learning from him not only knowledge, but also different skills and talents. I am glad that I worked under his supervision.

My deep thanks should be also extended to Prof. Andres Lepage for his support as a co-advisor since my first day in the research. Dr. Lepage has been directing me to the most powerful source of knowledge. I really appreciate his unlimited support and time in the numerical issues and other concepts. It was my pleasure to work with him and to learn from his experience.

During my research work I was assisted by great colleagues from the beginning. Special thanks for those from whom I have been helped in doing experiments and starting my numerical work. I am very thankful to José Ricardo Ribeiro Amorim and Nathanaell Vinicius De Camargos Welter for their effort in fabricating the small-scale six-story structure.

I must express my gratitude and my love to my family: my parents Marshad Almarshad and Fatimah Alrobaish and to my wife Areej Aldubaykhi and my sibling Ziad, whom without this work would not be completed. Thank you for standing with me during the past years. My daughters Holall and Rouwd have been the joy of my life.

The writer also wants to express his appreciation for his sponsor Qassim University. Their support and funding is highly acknowledged. Thank you for providing me the chance to complete my graduate degree.

Table of Contents

LIST OF FIGURES

LIST OF EQUATIONS

LIST OF TABLES

CHAPTER 1: INTRODUCTION

Story drift (SD), which is the relative displacement between two successive building floors, and story drift ratio (SDR), defined as the SD divided by the story height, are important indicators of structural damage and integrity [1]. One of the main goals of structural health monitoring (SHM) is to detect structural damage prior to critical events, such as major structural deterioration and failure, to provide needed assessment after a damaging event, such as an earthquake. Building codes limit the maximum allowable SDR based on the occupancy category of the building structure [1].

Measuring displacements of structures during earthquakes is a challenging task. Direct measurement approaches using displacement sensors such as Linear Variable Differential Transformers (LVDT), dial gauges, and string pots require a fixed reference point for installing these sensors, which is likely unavailable in the field [2]. Converting acceleration measurement into displacement through double integration does not provide a reliable solution in many cases due to the unknown initial conditions and unavoidable noise in the acceleration measurement. Moreover, the correction process that is applied to the estimated displacement from acceleration is likely to remove some critical information, which then leads to missing some of the displacement components, generally the low frequency components of structural movement [3].

Different techniques have been developed to estimate displacements from acceleration measurements. One of these approaches was proposed by Lee, et al. (2010) by approximating the acceleration measurements as a second-order central finite difference of the displacement. The displacement is reconstructed by minimizing the least-squared errors between the approximated acceleration and the measured acceleration [2]. Their proposed method is a Finite Impulse

Response (FIR) filter method formulated in the time domain. Therefore, it is referred to as the time-domain FIR filter method in this study. Lee et al, [2] stated that applying the moving-time window leads to missing parts of the reconstructed displacement at the boundaries of the displacement record (beginning and end of the record). The missing parts might be critical, especially the beginning part because in some of the events the peak displacement happens during the initial part.

Besides acceleration measurements, strain measurements have also been used to reconstruct displacements. The process relies on the displacement mode shapes and strain mode shapes, which are both mass-normalized, to convert strain to displacement. However, in practical applications, identifying mass-normalized mode shapes is challenging in building structures mainly because of the need to measure the output at the same location of the input [4].

This study has two main objectives. The first objective is to enhance the time-domain FIR filter method to estimate the structural displacement from acceleration by recovering the missing part at the boundaries of the displacement record. The missing part is recovered by applying the Zero-Padding Technique. The second objective is to study the feasibility of estimating displacement of frame structures using strain measurements. The proposed method does not require using the mass-normalized mode shapes for building structures from linear response. Instead, the arbitrarily scaled mode shapes are re-scaled based on the modal participation mass ratios, which are then used in estimating the displacement. The estimated displacement is further scaled using a factor obtained from the acceleration measurement. The modal participation mass ratios can be estimated using an assumed mass matrix which is proportional to the actual mass matrix, based on the observation that building structures generally have uniformly distributed mass through its height. The proposed research consists of two phases. The first phase is a numerical

investigation of displacement estimation algorithms. The second phase is an experimental validation based on shake table tests with a small-scale multi-story structure.

Chapter 2 provides the background and a literature review about previous studies related to displacement of structures and displacement estimation from acceleration and strain measurements. This chapter includes a discussion about the unrealistic drift sources in the estimated displacement from acceleration measurements. In addition, there is a literature review about correction methods.

Chapter 3 shows the details in design, construction, numerical modeling, system identification, and model calibration of a small-scale six-story structure. This chapter contains the details of the two numerical models that are used in this study to identify dynamic properties of the physical model.

Chapter 4 contains the main contributions of this study. It introduces methods to estimate displacement for building structures from acceleration measurements, strain measurements, and combined acceleration and strain measurements. The estimation of displacement from strain is applied to the small-scale six-story structure based on a numerical model. In addition, a method is proposed in this chapter to overcome the difficulty of using the mass-normalized mode shapes for building structures.

Chapter 5 presents the conclusion of this study and a discussion about future work, including the need for improving the displacement estimation accuracy and exploring its potential use for cases that involve nonlinear response.

CHAPTER 2: RESEARCH BACKGROUND

This chapter presents a background of the research related to displacement estimation of structures. The first section is a review for estimating displacement from acceleration measurements. The second section is a review for using strain measurements to estimate the displacements of structures.

For Structural Health Monitoring (SHM), structural displacement response might contain information directly related to structural integrity. For example, during a strong ground motion, a practical and quick decision regarding structural damage and integrity can be taken based on the maximum displacement of the structure [2].

2.1. Displacement Estimation from Acceleration Measurements

Estimating displacement from acceleration measurements is a common method due to its simplicity, relatively lower cost than other direct approaches, and reasonable outcomes in most cases. In addition, the accelerometers do not require a fixed reference point as most direct measurements do [3].

Converting acceleration measurements into displacement can be achieved by different methods. Different issues have been noticed by applying different methods as well. For example, one of the common methods is double integration of acceleration to obtain displacement. The integration method usually leads to unrealistic calculated values of the velocity and displacement. Many researchers have tried to identify the sources of these unrealistic values and other researchers have tried to provide multiple solutions to overcome this anomaly.

In 1947, Housner published a study about computing ground displacement from recorded acceleration measurements. He also used records obtained from displacement meters during the 1933 Los Angeles earthquake at the Subway Terminal station as reference signals [5]. Housner attributed the unrealistic drift in the computed displacement (from acceleration measurements) to not recording both the initial shock of the ground motion (late triggering) and the baseline on the accelerograph. He suggested establishing a baseline correction scheme for integration purposes. Housner emphasized that the computed displacement will lose some of its sharpness [5].

In 2010, Skolnik and Wallace published a study about the assessment of the story drift measurements [1]. Skolnik and Wallace argue that obtaining the story drift from acceleration measurements through double integration is challenging and that there are several problems in applying this method including signal processing procedures and the instrumentation limitations. According to Skolnik and Wallace, double integration of the acceleration measurements to obtain the displacement involves sensitive and subjective signal processing procedures, such as the baseline correction, zero value at the end of the signal, and the band-pass filtering processes. They suggest improving the signal quality by applying low-pass filtering and an initial baseline correction prior to the numerical integration. As a result of the surrounding conditions (e.g., change in the temperature), the data are noisy and most likely will have a constant offset, which can be corrected by subtracting the constant value from the raw data. The low-pass filter helps in reducing the noise amplitude, where it generally appears in the high frequency bandwidth. Their conclusions state that the error in the estimated displacement obtained from double integration of linear-response acceleration can be as low as 5% of the peak value; however, for nonlinear response the error might be higher than 12% and the residual displacement will be eliminated [1].

2.1.1. Drift sources in double integrated acceleration and correction methods

It is known that after the integration of acceleration measurements a drift appears in the calculated displacement due to unknown initial conditions and other sources such as measurement noise. This visible error is partly due to digitization and all other errors aggravate with an increase of time and amplify after integration [6]. Other causes that were mentioned by Yang, et al. [7] are the offset in the acceleration data due to electrical hysteresis or mechanical hysteresis in the sensors. A small offset in the data can introduce a drift in the calculated displacement. Growth of random noise is another source that leads to the unrealistic drift after integration. Noise in accelerometers can come from transistor noise or thermal-mechanical noise [8].

Noise level in the acceleration measurements can vary based on the type of accelerometers used. According to the study by Iwan et al. [6] there is a marked difference between the analog and digital systems in term of the noise level. This difference in level is close to two orders of magnitude at low frequency components (long periods) and it is more than one order of magnitude for high frequency components (short periods). He also states that the digital instruments have more capability and accuracy than the analog instruments, especially in events that are short in time. Iwan et al. also mentioned that acceleration data from digital instruments should give improved results when integrating recorded acceleration to obtain displacement and velocity [6].

In 2003, Boore published a paper that discusses the error introduced by the conversion of the analog data to digital data [9]. In addition to the other error sources, such as the ground tilt in the elastic zone, inelastic deformation of the ground, the misalignment of orthogonal sensors, which cause cross feed, and the instruments hysteresis, Boore argues that the steps in the analog-

to-digital conversion can introduce pulses in the output. Furthermore, the offsets in the acceleration baseline can cause major deviations in the estimated displacement [9].

2.1.2. Baseline correction methods and filtering

Different methods have been proposed to eliminate the unrealistic drift that results from double integration of acceleration records. Due to variety of the drift sources there are different approaches to correct it. Baseline correction is one of the most common methods. In 1961, Berg and Housner [10] published a study that discusses the integrated velocity and displacement from acceleration recorded during strong ground motion. They show several examples from different earthquakes where they integrated the velocity and displacement from recorded acceleration. In order to integrate the acceleration measurements, they assumed the initial velocity and displacement to be zero and they used a temporary straight base line, as they called it, where they performed a technique to come up with the base line for the acceleration measurements. One of their examples was the Pasadena earthquake of July 21, 1952. They performed their study on this example based on the accelerometer data from the California Institute of Technology; in addition, they have the recorded displacement for the same location. Berg and Housner compared their integrated displacement with the recorded displacement, and they noticed a reasonable agreement between the two. They argued that the deviations between the two were due to the instruments' limitations [10].

Trifunac in 1971 proposed a baseline correction approach in addition to applying high pass filtering to uncorrected digitized acceleration measurements [11]. Trifunac compared his new approach to the classical parabolic baseline correction. In his conclusions, he argues that the new

proposed method should be more accurate regardless of the record length. While the accuracy of the classical parabolic correction is affected directly by the length of the record [11].

In 1985, Iwan et al. proposed a baseline correction scheme by removing two baselines from two different time locations t_1 and t_2. The t_1 is the time step where the acceleration exceeds 50 cm/s2, while t_2 can be taken either after the acceleration never exceeds the 50 cm/s^2 or it can be taken as a value to minimize the final displacement [6]. Boore adopted the scheme by Iwan et al. arguing that most of the velocities derived from uncorrected acceleration data from the 1999 Chi-Chi earthquake showed a linear trend for systems with long periods of vibrations. In Boore's approach, t_2 can be taken as any value after t_1. According to Boore, structures that have a period less than 20 sec should not be sensitive to baseline correction schemes [12].

An alternative approach for baseline correction was proposed by Yang et al. [7]. They proposed conducting a baseline correction in the time domain for the acceleration measurements before the integration by using the least-square curve fitting technique, and then conducting further processing in the frequency domain by applying a window filtering to remove the sources of low frequency components in the integrated acceleration. By applying the approach by Yang et al. to the acceleration measurements, the derived velocity and displacement should be realistic. In addition, they compared their approach with that by Trifunac [11] and several other schemes, and their approach provided better results in their case studies [7].

Filtering acceleration measurements is another common technique used to improve the accuracy of the estimated displacement. Filtering is generally used to remove high frequency components (low-pass filter) [11] or low frequency components (high-pass filter). Filtering has been widely used in combination with baseline correction or use of filtering alone provides major improvement in the accuracy of the estimated displacement [3] and [2].

2.2. Displacement Estimation from Strain Measurements

Converting strain measurements to displacement through the displacement-strain mode shape relationship is commonly applied to estimate dynamic displacement in different fields [13, 14]. For example, research has been conducted in Aerospace Engineering to estimate the displacements of airplane wings.

One of the early researchers that discussed converting strain measurements to displacement measurements was Foss and Haugse in 1995 [13]. Foss and Haugse discussed some major challenges in using strain measurements such as the strain level is low in terms of the amplitude that usually reached from the modal excitation sources, which affect the frequency response function (FRF) as well. They also compared the signal to noise level ratios between accelerometers, where the accelerometers' noise ratio is better than the strains' noise ratio. It is known that the strain measurements can vary from a microscale to almost nonexistent. Foss and Haugse stated that it is hard to achieve an accuracy below 10 microstrain. Different factors can affect the accuracy of the strain gauges; for example, a neighboring radio station can affect the strain measurements. Another factor that might have an impact on the strain gauges is the surrounding temperature. Any random movement of environment room air may lead to large output. Sometimes strain gauges require a long time to reach the equilibrium since they are self-generators of heat. Accuracy of the strain measurements have a direct relationship to the quality of the attachment, where if the bond has a poor quality or does not cover the required area, the output will very likely be flawed [13]. Foss and Haugse developed a method that converts strain measurements to displacement by using a transformation matrix that can be derived from mass-

normalized mode shapes of the displacement and strain. They validated their method experimentally using a cantilever plate [13].

Similarly, Pisoni et al. in 1995 proposed a method to convert strain measurements to displacement [14]. Their method is based on identifying the displacement mode shapes – by performing modal analysis – and the transfer function to estimate some parameters, to define the displacement as a function of strain and mode shapes. Pisoni et al. performed an experimental study consisting of a free vibration of a clamped-end beam to derive the displacement using strain measurements. They measured the displacement and compared it with calculated displacement using their method. They found reasonable agreement between the measured and the calculated displacements after the high frequency components in the strain signal died out. However, before the high frequency in the strain signal died out the calculated displacement was overestimated. The reason of the overestimation, according to Pisoni et al., was due to strain data having higher dynamic sensitivity when compared with displacement data. They filtered the strain data by eliminating all frequencies higher than 200 Hz, which showed improvements in the accuracy of the calculated displacements [14].

Kang et al. published a study in 2007 showing the effectiveness of converting Fiber Bragg grating (FBG) strain sensors measurements to dynamic displacement by using the modal analysis properties [15]. Bragg grating (FBG) strain sensors were chosen in their study due to their multiplexing ability. They applied different loadings on an aluminum and acryl beam specimens in their experimental porgram. Their study involved mass-normalized mode shapes in their estimation, which is similar to what other previous researchers had done. They obtained the mass-normalized mode shapes by performing a shaker test. Their objective was to obtain the whole deformation of structures using FBG strain sensors [15].

Park et al. 2013 proposed an approach for estimating displacement of bridges by combining acceleration and strain measurements [3]. Their objective was to estimate nonzero mean dynamic displacement to preserve the pseudo-static displacement of bridges under traffic loading. The acceleration measurements are used to estimate the displacement by double integration followed by a high-pass filtering and assuming a zero-mean process. However, zero mean eliminates the pseudo-static displacement. On the other hand, there is a difficulty in using strain for high-frequency modes. According to Park et al., the fusion of acceleration and strain measurements was able to estimate accurately a nonzero mean displacement. They have conducted both numerical and experimental investigation to support the validity of their approach [3].

In 2014, Wang et al. published a study based on strain mode shapes to estimate the displacement using stain measurements for beam structures [16]. Their approach is based on the displacement-strain relation and uses the displacement and strain mode shapes. They use the cross-correlation function of the measured strain to estimate the strain mode shapes. They have conducted numerical and experimental investigations on a simply supported beam that was subjected to impulse and earthquake loading. This study shows displacement estimation of a simply supported beam at any location based on strain measurements with about 7% error [16].

2.3. Response Error Estimation

Different methods have been developed to quantify the error between the measured and estimated responses. One of the most common methods is the root-mean-square (RMS) error, where the error is estimated based on the RMS value from difference between of the reference and the estimated signals over the RMS of the reference signal.

An alternative approach to quantify the error between measured and estimated signals was proposed by Dragovich and Lepage in 2009 [17]. The approach was termed the frequency domain error (FDE) index. The FDE index varies between 0 and 1, where 0 means no error. The FDE index is calculated based on the Fourier spectra of the calculated and measured signals. The index relies on the fast Fourier transform (FFT). The main advantage of the FDE index in comparison to the RMS error is its ability to distinguish between the amplitude error and the phase error. The RMS error is not able to distinguish between phase and amplitude errors.

2.4. Summary

The estimated displacement from double integrating the raw acceleration measurements will is prone to an unrealistic drift that might be due to one or more of the following:

- Unknown initial conditions
- Unrecorded baseline
- Digitization processes
- Electrical or mechanical hysteresis in the sensors
- Random measurement noise

Several assumptions are typically made to estimate displacement from acceleration measurements, such as:

- Zero initial conditions for the structure
- Zero value at the end of the estimated displacement
- The mean value to be zero for the estimated displacement

These assumptions combined with signal processing have a direct impact on the accuracy of the estimated displacement. The residual displacement is typically eliminated through signal processing steps. Filtering low and high frequency components may prove to be critical.

Estimating the dynamic displacement from strain measurements has been used for different applications. Strain measurements are mostly converted to displacement by getting the advantage of the modal analysis properties. The procedure for converting strain measurements typically use a transformation matrix, which converts the strain measurements to displacement, from the mass-normalized mode shapes. Difficulty in obtaining the mass-normalized mode shapes limits this approach. To overcome the need for mass-normalized mode shapes this study will evaluate the use of the modal participation mass ratios combined with a scaling factor α factor.

CHAPTER 3: EXPERIMENTS AND NUMERICAL SIMULATION USING A SMALL-SCALE STRUCTURE

3.1. Design and Construction of a Small-Scale Six-Story Structure

To perform numerical simulation and experimental investigation, a small-scale six-story steel structure is designed with a total height of 74.25 inches. Each story is designed to be 1 foot tall (Figure 3-1). The structure is made completely from steel and assembled by angles, bolts, and nuts.

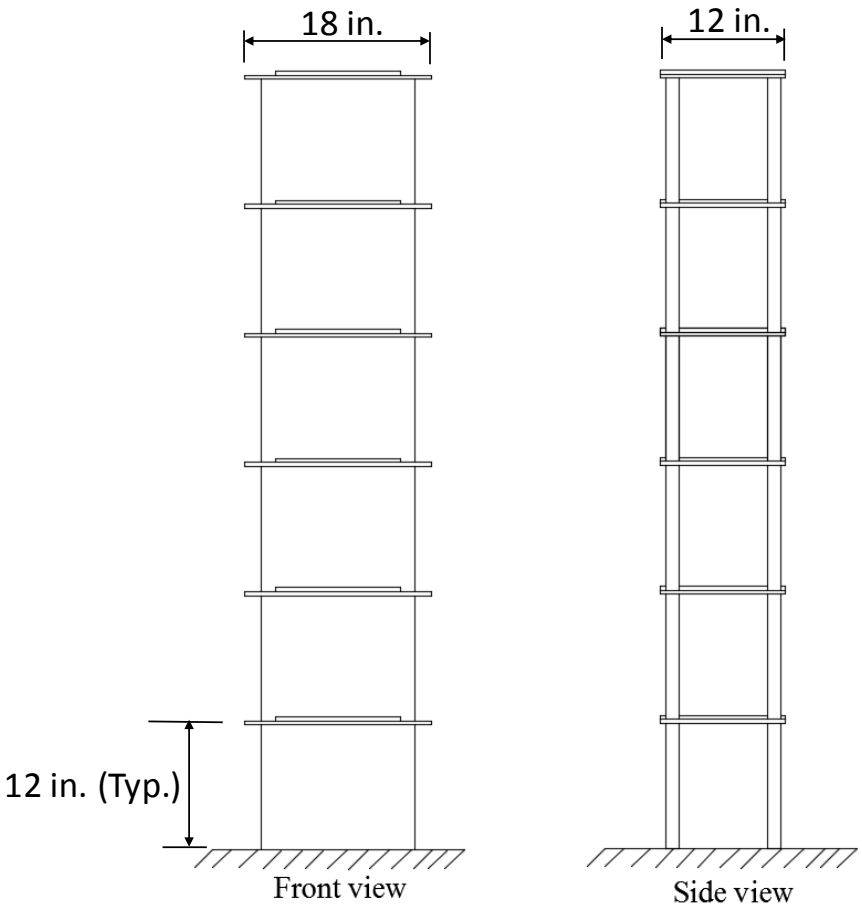

Figure 3-1: Front and side view of the small-scale six-story structure

Columns of the structure are spring steel (or it called Blue Steel) with $1\frac{1}{4}$ in. width and $\frac{1}{8}$ in. thickness. These columns are connected to two $\frac{3}{8}$ plates using two angles at each end with one bolt between the column and the angles. Two bolts are connecting each angel to the plate (Figure 3-2).

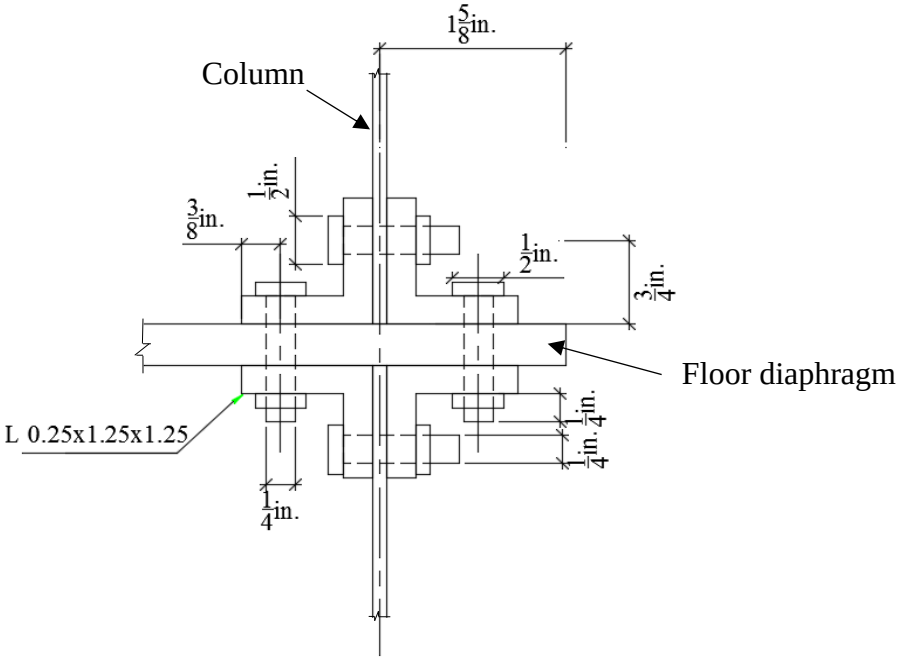

Figure 3-2: Typical connection detail

Floor diaphragms are formed from an 18 in. by 12 in. plate with thickness of $\frac{3}{8}$ in. and a 12 in. by 12 in. plate with thickness of $\frac{3}{8}$ in. as shown in Figure 3-3 and Figure 3-4. The two plates for each story are connected by four large bolts. The second plate is to add additional mass to the structure to achieve the target dynamic properties.

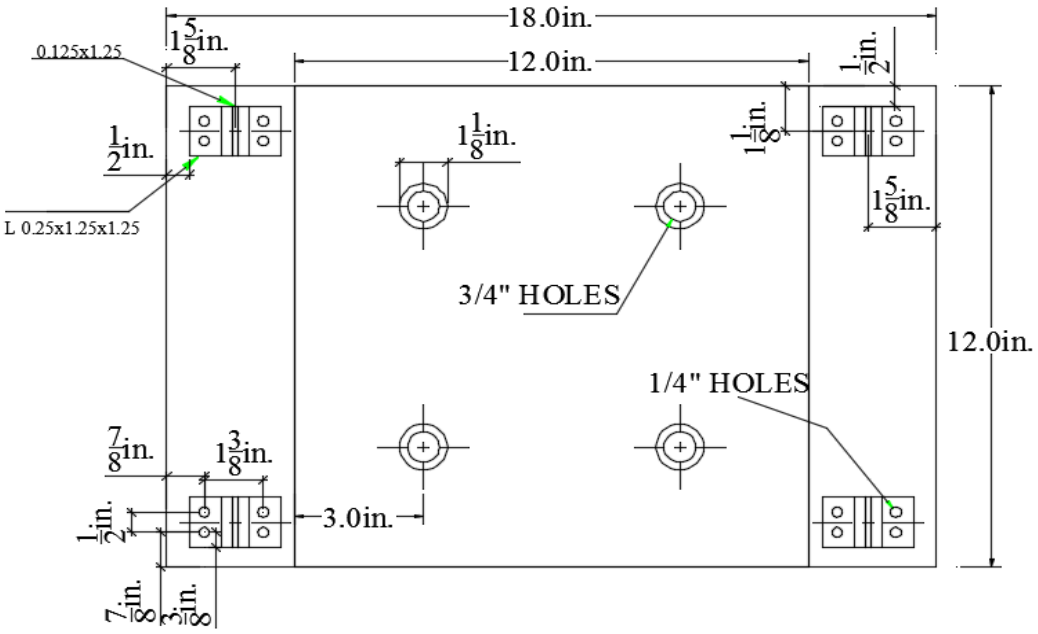

Figure 3-3: Floor diaphragm plan view

Columns are attached to two angles at each end as shown in Figure 3-4. Each angle is connected to the plates using two bolts and it is further connected with the column by one bolt in the middle. The connections were designed without any gap between the column and the angles to ensure the rigidity, as possible. A rectangular thick plate with dimensions of 18 inches by 24 inches was designed to be used as the base of the structure. Using this base plate the structure will be attached to the shake table for testing.

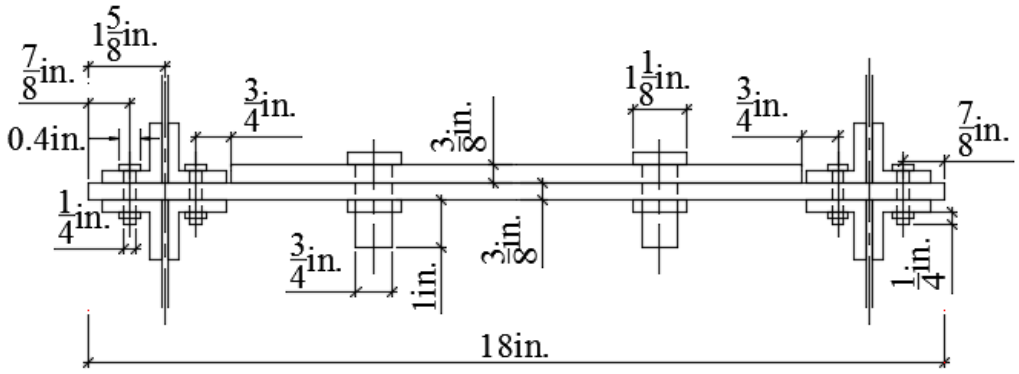

Figure 3-4: Floor diaphragm elevation

The designed structure was constructed using the same designed dimensions and material properties (Figure 3-5). The process was started by fabricating the angles and columns to the designed length and drilling the holes into columns. Then the plates were marked and drilled to install eight angles at each side except for the roof and the base plates, which they have angles at only one side.

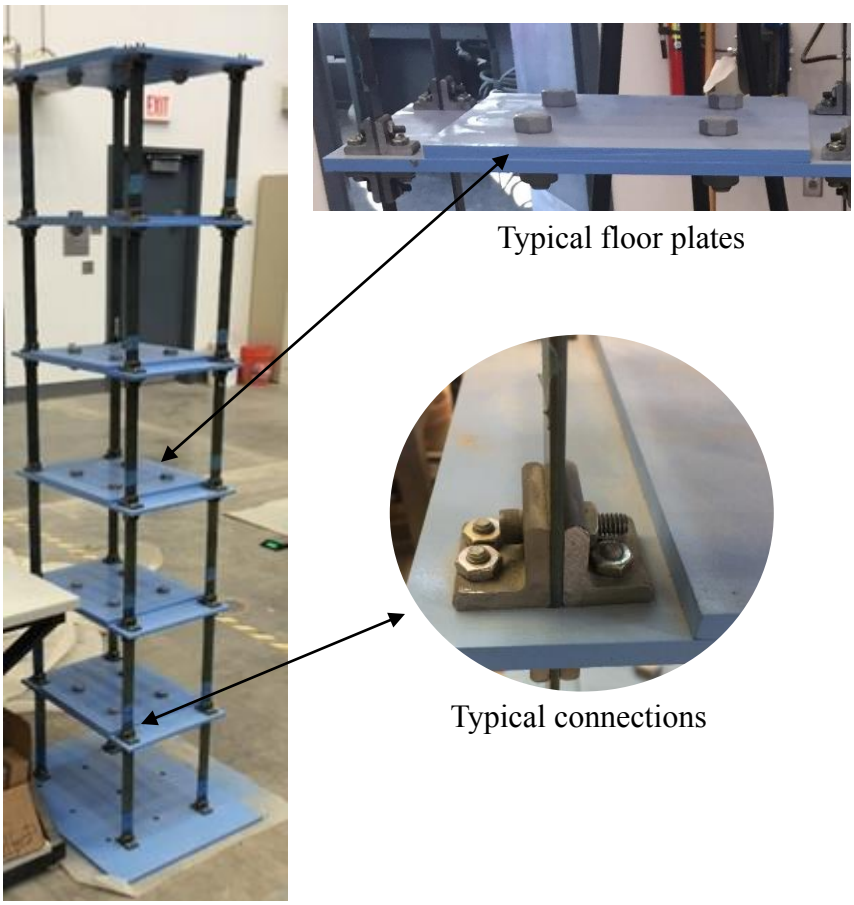

Figure 3-5: The constructed small-scale six-story structure

After the preliminary assembly, the structure was disassembled for painting. After the painting processes were completed the structure's components were weighted on a scale to obtain the exact weight of the structure for numerical modeling purposes. The weight of the small-scale

six-story structure is 267.5 pounds in total, which includes the large and the small plates, columns, angles, and all bolts with nuts.

The structure is then attached to a shake table in the West Campus Structural Laboratory at The University of Kansas (Figure 3-6). The structure then will be used to perform experiments with the shake table. System identification using the shake table is discussed in section 3.3 and other experimental results are discussed in section 4.2.4. The shake table will be used to simulate different input signals especially that of earthquakes.

Figure 3-6: The structure mounted on the shake table in the structural engineering laboratory at The University of Kansas

3.2. Numerical Modeling

Two numerical models of the small-scale six-story structure are built in SAP 2000 to simulate different responses (e.g., acceleration, displacement, and strain) of the structure under earthquake loading Figure 3-7. These numerical models were modeled to simulate the actual small-scale six-story structure model which is discussed in section 3.1. The small-scale model and the full numerical model are both six-story structures made from steel and attached to thin high strength columns using angels and bolts. The simulated responses will be used to assess displacement estimation from acceleration and strain measurements.

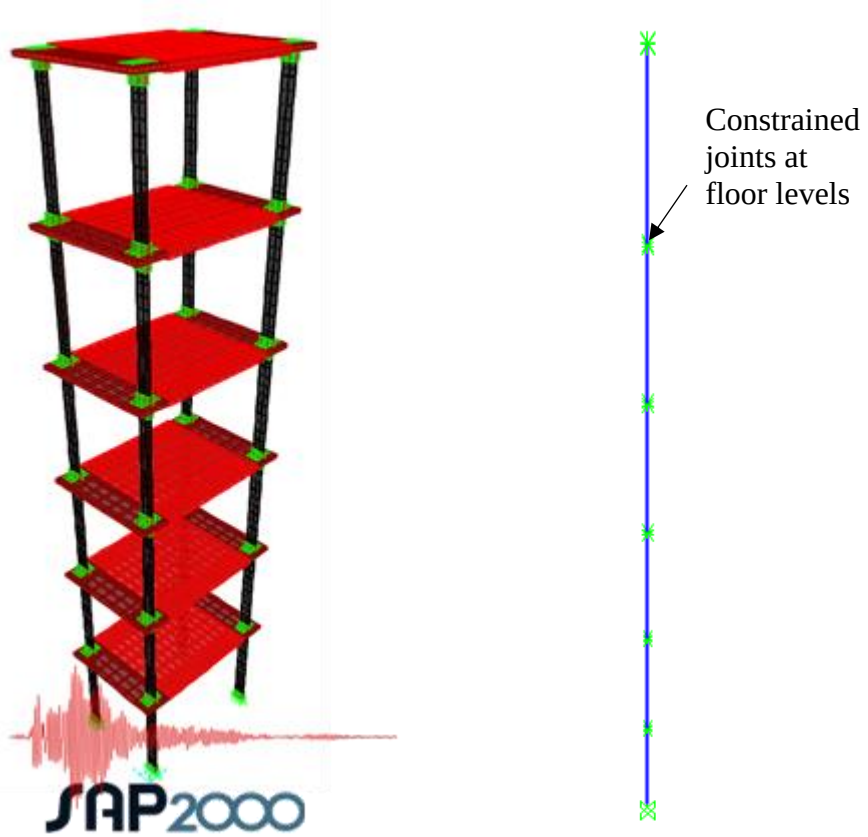

Figure 3-7: The full numerical model (left) and the simplified model (right)

The geometric details of the numerical model are the same as those of the physical model. Angle connections are represented in the numerical model, using thicker area elements than those used for columns. The mass of this structure is defined to be same as the actual mass of the small-scale six-story structure. The boundary conditions at the base of the structure were assigned to be fixed.

Another simplified numerical model was created in SAP2000 as shown in Figure 3-7. This simplified model represents a quarter of the full numerical model and it is modeled as a six beam elements with the same total height of the full model and quarter lumped mass at the nodes, where each node represents the floor level. Restrains are applied to the six nodes in all degree of freedoms except in one translational direction. This model is used for quick investigations and it has the same modal frequencies as the full numerical model. Stiffness of the floor diaphragm and connecting angles are represented through the equivalent rigid length offset. This simplified model is helpful in the calibration processes with the physical structure, which will be discussed in section 3.3. The comparison between natural frequencies of the full and the simplified model are given in Table 3-1. Based on this comparison the two models have the same natural frequencies, where the full model has full mass and stiffness, while the simplified model has a quarter of mass and stiffness since it represents a quarter of the structure.

3.3. System Identification and Calibration

Identification of the dynamic properties of the physical model is necessary in order to calibrate the numerical model. The method chosen for this study to perform system identification is applying Band-Limited White Noise (BLWN) to the small-scale six-story structure using the shake table (Figure 3-8). The dynamic properties are then identified based on the measured input and output signals.

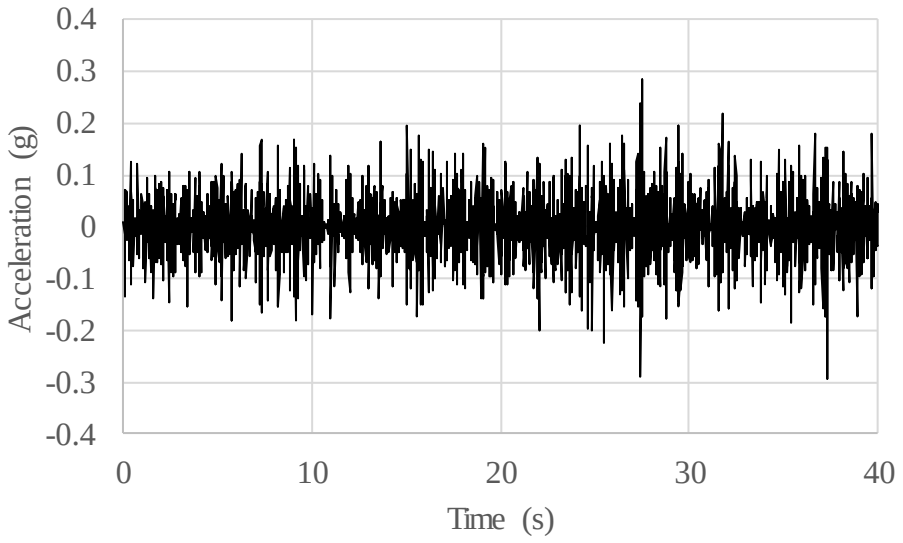

Figure 3-8: The input band-limited white noise

The acceleration data are collected using accelerometers installed at each floor. Eight accelerometers are used in total, including one accelerometer at each floor diaphragm and two at the base (Figure 3-9). Transfer function is estimated using the cross-power spectral density between the input (Figure 3-8) and the output. The estimated transfer function is shown in Figure 3-10 with six clear peaks; each peak represents one mode.

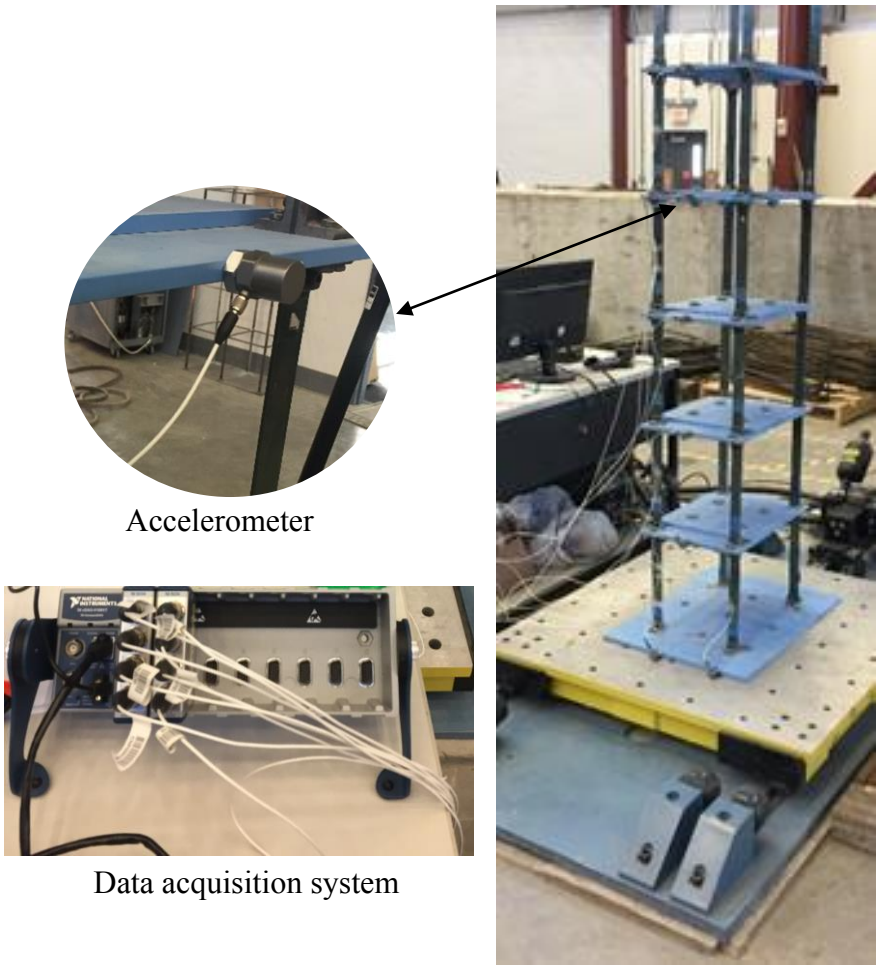

Figure 3-9: Accelerometers attached to the small-scale six-story structure

Using the transfer function in Figure 3-10, the natural frequencies were obtained as shown in Table 3-1. In addition, the mode shapes (Figure 3-11) and the damping ratio was estimated as well from the transfer function of the sixth floor. The transfer function was estimated based on the measured acceleration from the sixth floor and the input excitation. The sixth floor is used here since it have clear peaks in comparison to the other floor measurements. The damping ratio of the fundamental mode is 2%. The identified properties will be used in the calibration processes.

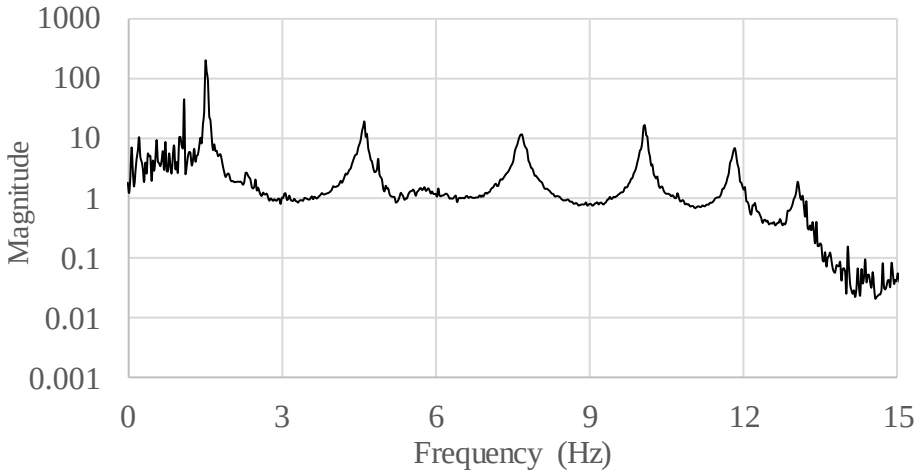

Figure 3-10: Transfer function of the small-scale six-story structure

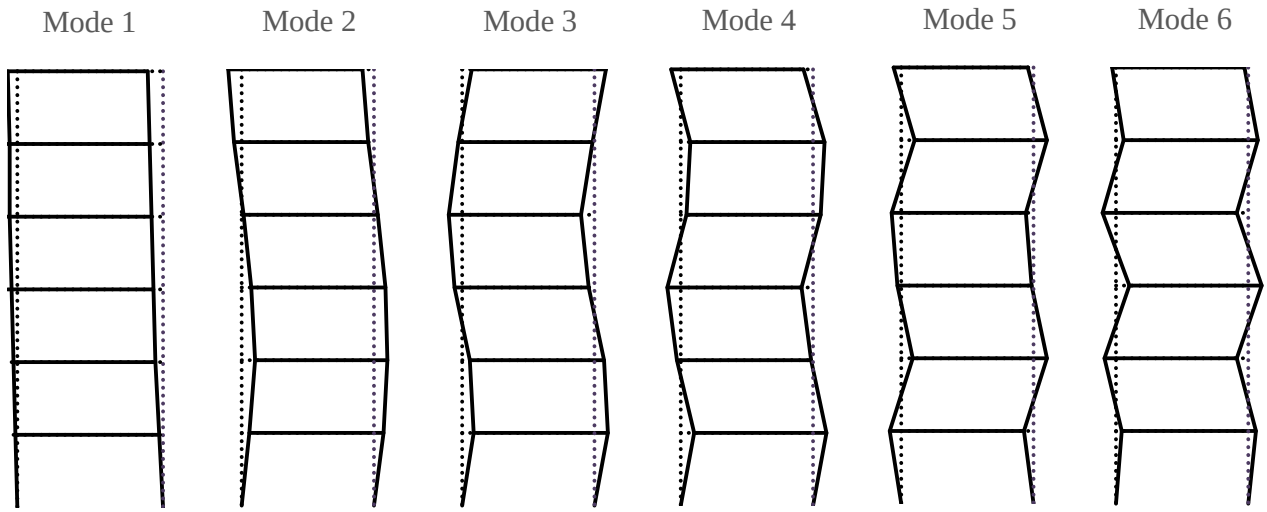

Figure 3-11: Identified mode shapes of the small-scale six-story structure

After identifying the natural frequencies of the physical model using the output from the applied BLWN test, the numerical models were calibrated to match the natural frequencies of the physical model. The numerical models show higher stiffness than the physical model due to the semi-rigid angle connections in the small-scale six-story structure. Since the angles are connected to the columns using one single bolt, they have lower stiffness than the numerical model which was modeled as fully rigged connections. In order to calibrate the numerical models stiffness to

the physical stiffness, the connection zone factor of the rigid length offset in the simplified model was reduced to be 36% instead of full rigid zone factor. For the full numerical model, the connection zone length was also changed to be 25% of the full connection zone length. Comparison between the physical model and the two numerical models is shown in Table 3-1. Identified damping ratios also shown in Table 3-1 for all six modes.

Table 3-1: Damping ratios and natural frequencies of the physical and numerical models before and after calibration

	Damping ratio %	Frequency (Hz)				
	The small-scale structure	The small-scale structure	Before the calibration		After the calibration	
			The full model	The simplified model	The full model	The simplified model
1st mode	2.0	1.5	1.9	1.9	1.5	1.5
2nd mode	0.6	4.6	5.6	5.6	4.5	4.5
3rd mode	0.8	7.6	9	9	7.3	7.3
4th mode	0.6	10	11.9	11.9	9.7	9.6
5th mode	0.4	11.8	14	14	11.5	11.3
6th mode	0.2	13	15.4	15.3	12.6	12.3

3.4. Summary

In this chapter, the design and fabrication details of the small-scale six-story structure were discussed. The system identification process of the small-scale six-story structure using BLWN excitation was explained. The natural frequencies, mode shapes, as well as the damping ratios were identified. The numerical models modeling details were described and the calibration process by reducing the connections stiffness was explained. The calibration process was based on calibrating the stiffness of the connections, while other details such as the geometric details and the masses were implemented to be the same as those of small-scale six-story structure. The numerical models

and the small-scale six-story structure will be used to perform numerical and experimental investigations in chapter 4.

CHAPTER 4: DISPLACEMENT ESTIMATION FROM LINEAR RESPONSE

4.1. Introduction

This chapter presents several different displacement estimation methods from linear structural response using two different types of measurements. The methods presented in the first part use acceleration measurements. Three methods are presented including double integration method, time-domain FIR filter method, and the proposed modification to the time-domain FIR filter method. The second part presents a preliminary investigation on combing acceleration and strain measurements through data fusion.

4.2. Displacement Estimation Using Acceleration Measurements

4.2.1. Double integration method

Double integration has been widely used in converting acceleration measurements to displacement. Integrating acceleration $\ddot{u}(t)$ over time produces a velocity time series $\dot{u}(t)$ and further integrating velocity over time yields a displacement time series $u(t)$, where *t* is the time vector as shown in equations (4-1) and (4-2).

$$\dot{u}(t) = \int_0^t \ddot{u}(t)dt, \tag{4-1}$$

$$u(t) = \int_0^t \dot{u}(t)dt, \tag{4-2}$$

Calculating structural displacement through double integration of acceleration is a common method in structural engineering because it is simple, less expensive, and does not require a fixed

reference point. In contrast, direct approaches such as using Linear Variable Differential Transformers (LVDT) sensors, are more expensive, more complicated and it requires a fixed reference point. A fixed reference point is hard to establish in many cases especially for large-scale structures. For this reason, in some cases reference-based displacement is not available, such as bridges and buildings, and the direct measurements sensors cannot be used [18]. Furthermore, in the case of both the structure and the reference fixed point are moving, the conditions for applying direct displacement measurement sensors, which is a fixed reference point, are not available [2].

However, one known issue of the double integration method is the unrealistic drift that appears in the estimated displacement after double integration of acceleration, as illustrated in Figure 4-1. The shown displacement in Figure 4-1 is obtained by double integrating the ground acceleration of El Centro 1940 NS. The velocity obtained from the integrated acceleration measurements in Figure 4-1 clearly has a constant shift, which causes a linear drift after integrating the velocity to obtain displacement. The unrealistic drift in the estimated displacement can be attributed to unknown initial conditions and the accumulation of measurements noise [5, 10].

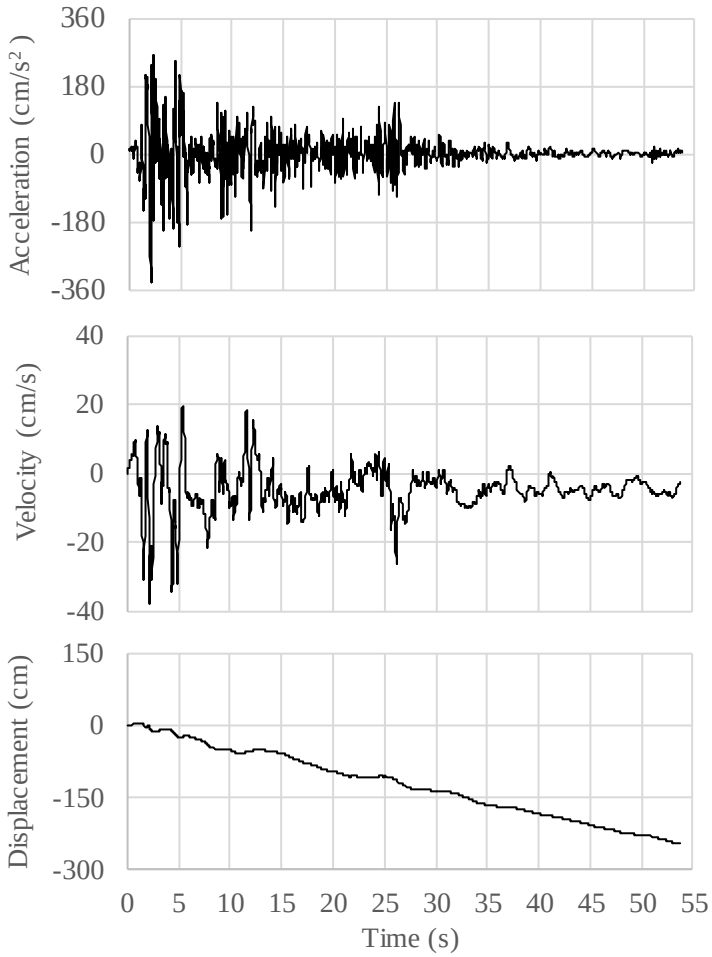

Figure 4-1: Displacement and velocity obtained from double integration of acceleration for El Centro 1940 NS

As shown in Figure 4-1, after integration a linear drift appears in the calculated displacement due to unknown initial conditions. Other causes that have been identified are the offset in the acceleration data due to electrical hysteresis or mechanical hysteresis in the sensors. Drift can appear even from a small offset in the acceleration data. Accumulation of random noise also causes unrealistic drift after integration [7].

Several approaches have been used to eliminate this drift. Since there are different causes of drift in the displacement and velocity measurements, there are different ways to eliminate it.

Filtering using a high-pass filter is commonly used to remove random noise that comes from accelerometers. However, filtering requires the selection of a cutoff frequency, which is subjective, and involves assumptions such as zero drift at the end of the displacement time history. This assumption may not be valid in practice, especially when a building experiences severe nonlinearities.

Based on numerical simulation, preliminary results for linear structural response indicated that double integration of acceleration, combined with high-pass filtering, is able to achieve relatively good results in the estimation of story drift. As shown in Figure 4-2, 5% random noise which represents the measurement noise was added to the data to simulate the real case.

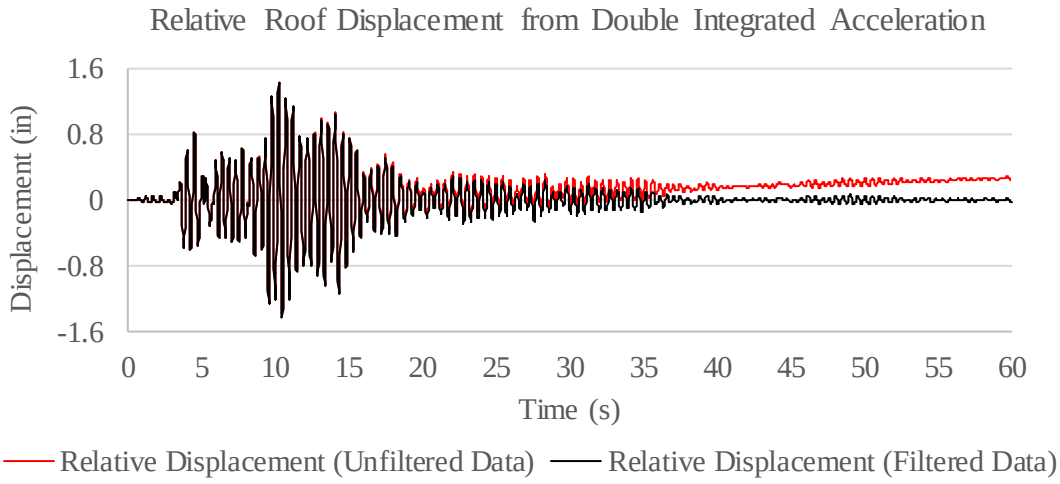

Figure 4-2: Filtered and unfiltered relative roof displacements, Burbank 1994 SW

Previous results were based on numerical simulation and added noise in combination with a high-pass filter. Applying high-pass filter only showed a good estimation of estimating story drift, so no further correction was needed. In case of estimating results from real acceleration measurements, filtering is not enough to eliminate the drift in the story displacement of the structure, since the unrealistic drift might be from the unknown initial conditions and not from the

measurements noise only. In addition, filtering may cause losing some important components from the data if the cutoff frequency was not chosen properly.

One additional correction approach widely used with filtering is baseline correction. One common correction scheme is to eliminate the drift in the estimated displacement by assuming zero displacement at the end of the record. Assuming zero displacement for structures after the end of an event might be correct for linear response. However, it may not be correct in the presence of nonlinearity. Such an assumption would eliminate the permanent displacement of a structure or of the ground, which sometimes is critical in evaluating damage and integrity of structures [1].

4.2.2. Time-domain finite impulse response (FIR) filter method

An alternative approach is proposed by Lee et al. [2] to design a finite impulse response (FIR) filter that can estimate displacement u from acceleration $\bar{a}$. Displacement u can be estimated by solving the following optimization problem:

$$\underset{u}{\text{Min}}\,\Pi = \frac{1}{2}\left\| L_a \left(L_c u - \Delta t^2 \bar{a} \right) \right\|_2^2 + \frac{\lambda^2}{2}\left\| u \right\|_2^2 \tag{4-3}$$

The solution to the minimization problem is expressed as:

$$u = \left(L^T L + \lambda^2 I \right)^{-1} L^T L_a \bar{a} \Delta t^2 \tag{4-4}$$

Where Δt is the sample time of the measured data, $L = L_a L_c$, L_a is a diagonal weighting matrix. L_a is a diagonal weighting matrix with dimension of (2k+1) by (2k+1), where k is the number of data points, with all diagonal entries of 1 except the last and first entries, which are equal to $1/\sqrt{2}$. L_c Equation (4-5) is the second-order differential operator matrix of the discretized trapezoidal rule with order (2k+1) by (2k+3) [2]. λ is a regularization factor for the minimization problem. Lee et

al. [2] suggests using an optimal regularization factor as $\lambda=46.81N_d^{-1.95}$, where N_d is the number of data points in the time window. The number of data points in the time window is suggested to be three times the fundamental period of the structure of interest [3].

$$\mathrm{Lc} = \begin{bmatrix} 1 & -2 & 1 & & & & \\ & 1 & -2 & 1 & & 0 & \\ & & & \ddots & & & \\ & 0 & & 1 & -2 & 1 & \\ & & & & 1 & -2 & 1 \end{bmatrix} \tag{4-5}$$

Lee et al. [2] also suggests using an overlapping moving time window technique (Figure 4-3) instead of using a non-overlapping time window to improve the accuracy of the reconstructed displacement. The non-overlapping time window reconstructs the displacement for the entire window size and moves forward by a window size length to the next time window. All data points in the time window are used as a solution for the reconstructed displacement. On the other hand, the overlapping moving time window uses only the middle point of the widow as a solution for the displacement and then the window moves forward by one data point to the next window. By applying the overlapping moving time window, the whole displacement is reconstructed except at the boundaries, the beginning and end parts, of the displacement record [2]. The key advantage of using the overlapping moving time window is avoiding the drawback coming from the boundaries in each window in the non-overlapping time window.

The missing parts at the boundaries of the displacement record are related to the size of the moving time window, since the missing part is the half of the window size at the beginning of the reconstructed displacement and half of the window size at the end boundary, so if the window size was two seconds, the first second and the last second of the reconstructed displacement will be missed. This happens because the way in which the moving window works as shown in Figure 4-3, where only the middle point of each window is reconstructed.

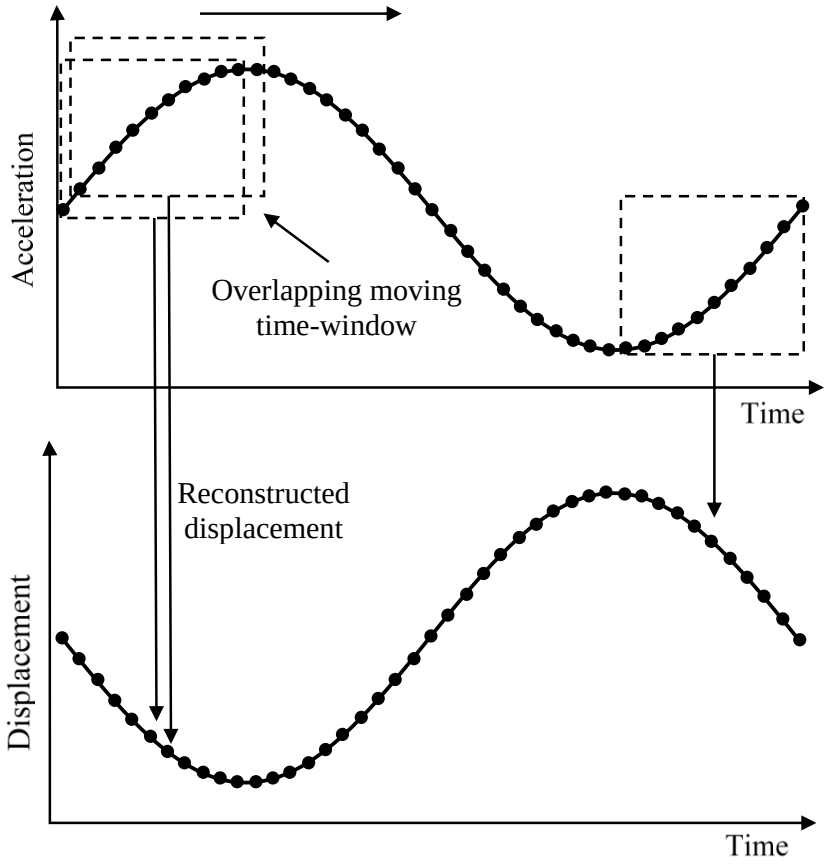

Figure 4-3: Moving time window

The size of the moving-time window has a direct effect on the accuracy of the reconstructed displacement. Larger windows give higher accuracy. According to Lee et al. [2], a window size that is longer than three times of the period of interest does not increase the solution accuracy. Based on their investigation, they have suggested using a window size three times the fundamental period of the structure [2]. Figure 4-5 illustrates how using a moving-time window will cause a loss in the calculated displacement at the beginning and the end of the displacement.

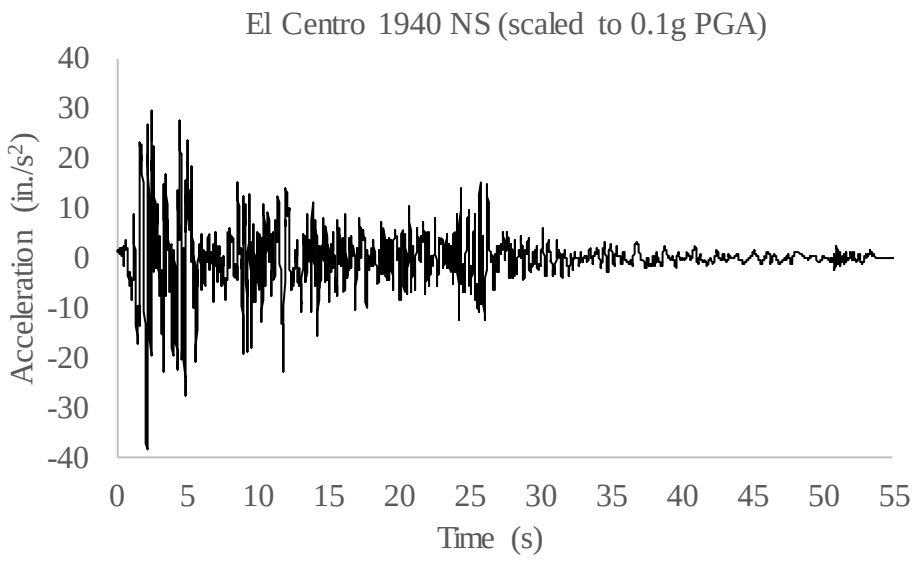

Figure 4-4: Scaled El Centro 1940 NS eathquake acceleration

The displacement shown in Figure 4-5 is the relative roof displacement of the numerical model discussed in chapter 3. The reference displacement was obtained from SAP2000 and the estimated displacement from acceleration measurements by applying the time-domain FIR filter method. The input ground motion for this case is the El Centro 1940 NS earthquake (Figure 4-4), which is scaled down to have a peak ground acceleration (PGA) of 0.1 g. The exact relative displacement from the numerical model in SAP2000 is also shown as the reference displacement in Figure 4-5.

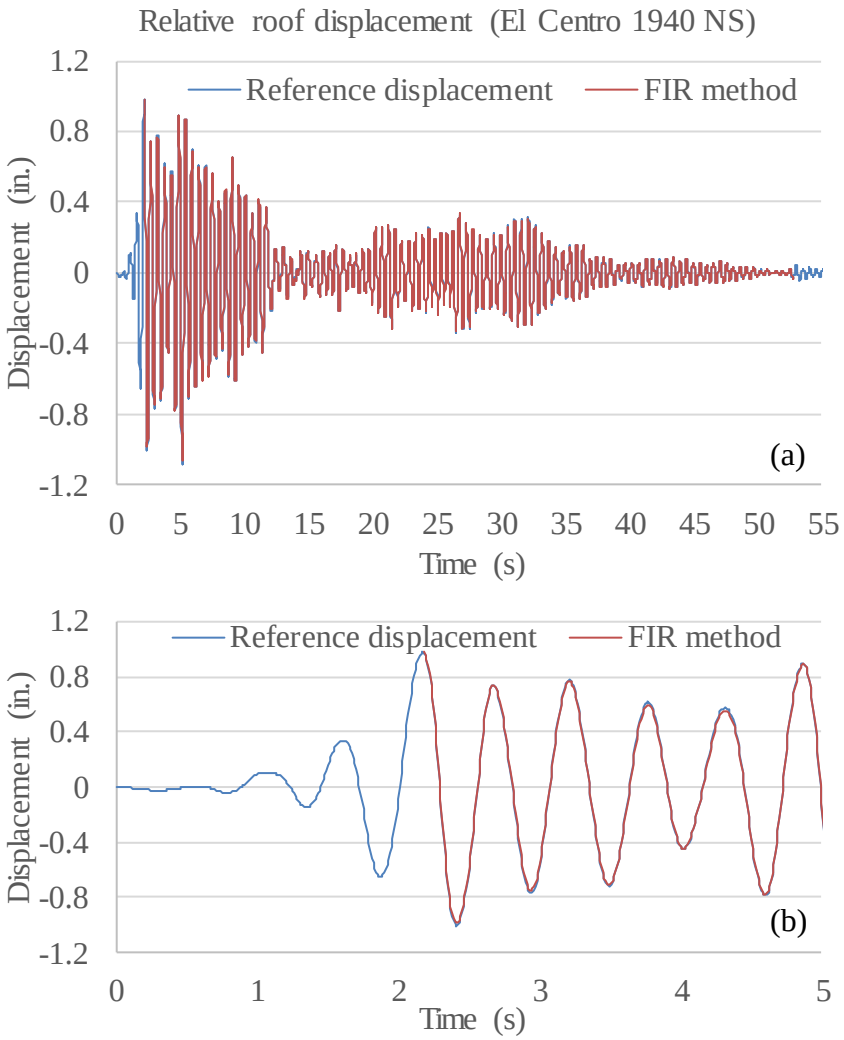

Figure 4-5: Relative roof displacement of the numerical model: (a) full record; (b) detailed comparison

As shown in Figure 4-5, the missing part at the boundaries of the solution might be significant, especially the beginning part. Some events have their highest energy at the beginning, such as the shown case from El Centro 1940 NS in Figure 4-5. As a result, missing such a part will have a significant effect on evaluation of the structure's response.

4.2.3. Proposed modification to the time-domain FIR filter method

The time-domain FIR filter method, which was discussed in 4.2.2, shows highly accurate displacement estimation except at the boundaries. Missing parts at boundaries might be significant, especially at the beginning, due to the energy level at the beginning of ground motion. For example, for the El Centro 1940 NS (Figure 4-4), the peak ground acceleration happened during the first two seconds. Missing the PGA will make the estimated displacement misleading.

To recover the missing displacement at the boundaries of the record, a modified moving-time window technique is proposed in this section. The moving-time window is modified by zero-padding the acceleration data at the beginning and the end, as shown in Figure 4-6. The length of padded zero points is equal to half of the window size. Zero-padding recovers the missing part at the beginning and at the end of a record by imaginary point before the record. The first reconstructed point of the displacement is the middle point of the time window.

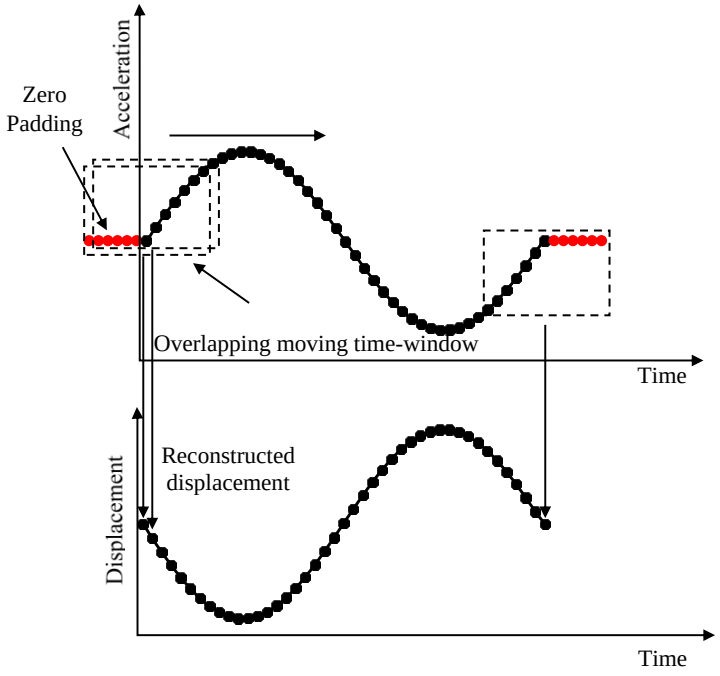

Figure 4-6: Moving time window with zero padding

The size of the window has a direct effect on the accuracy of the estimated displacement. A sensitivity test for the window size is shown in Figure 4-7 and Table 4-1 using the SAP2000 model and by applying two different earthquake records. Window size is related to the fundamental period of the structure by a factor which is multiplied to the fundamental period of the structure. The root-mean-square error was estimated using equation (4-6):

$$RMS\ Error = \left|\frac{RMS_{exact} - RMS_{est}}{RMS_{exact}}\right| \qquad (4\text{-}6)$$

Where RMS_{est} is the root mean square of the estimated displacement. RMS_{exact} is the root mean square of the reference displacement from SAP2000. Error can also be estimated by using different displacements with different window sizes until the difference, or the error, is acceptable.

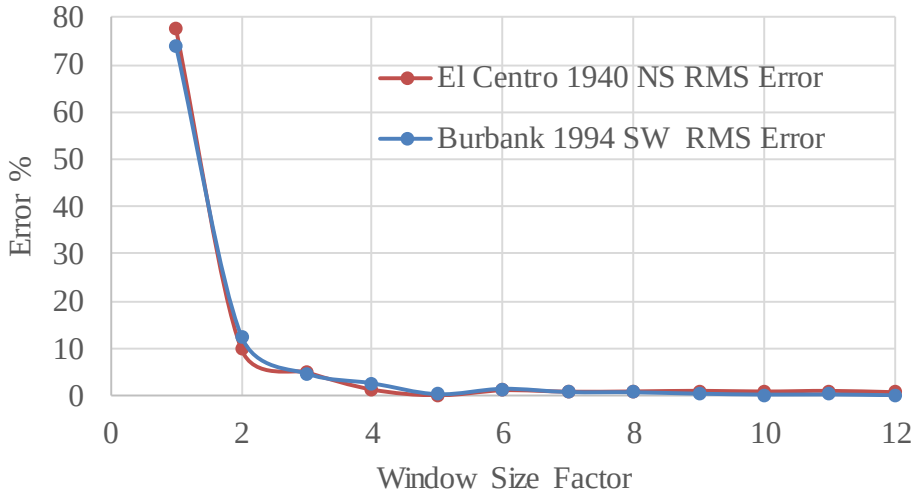

Figure 4-7: Window size factor sensitivity from numerical results

Based on the error shown in Figure 4-7 and Table 4-1, it is recommended to use a moving-time window with a length no less than four times the fundamental period of the structure. Applying a moving-time window that is shorter than four times of the period of interest may

underestimate the displacement. Using a moving-time window that is four to eight times the period of interest should produce accurate displacements.

Table 4-1: Effect of window size factor on the accuracy of the reconstructed displacement

Window size factor	RMS error El Centro 1940 NS	RMS error Burbank 1994 SW
2	0.0990	0.1261
4	0.0128	0.0260
6	0.0111	0.0143
8	0.0088	0.0070
10	0.0086	0.0021
12	0.0071	0.0007
14	0.0050	0.0001
16	0.0038	0.0027
18	0.0026	0.0028
20	0.0017	0.0029
25	0.0023	0.0002
40	0.0015	0.0025
50	0.0014	0.0017

The proposed method with the modified moving-time window technique was applied on the same case in Figure 4-4 and Figure 4-5. The zero-padding technique was able to recover the missing parts of the record, as shown in Figure 4-8. The estimated relative displacement using the proposed modification to the time-domain FIR filter method shows high accuracy in this numerical investigation.

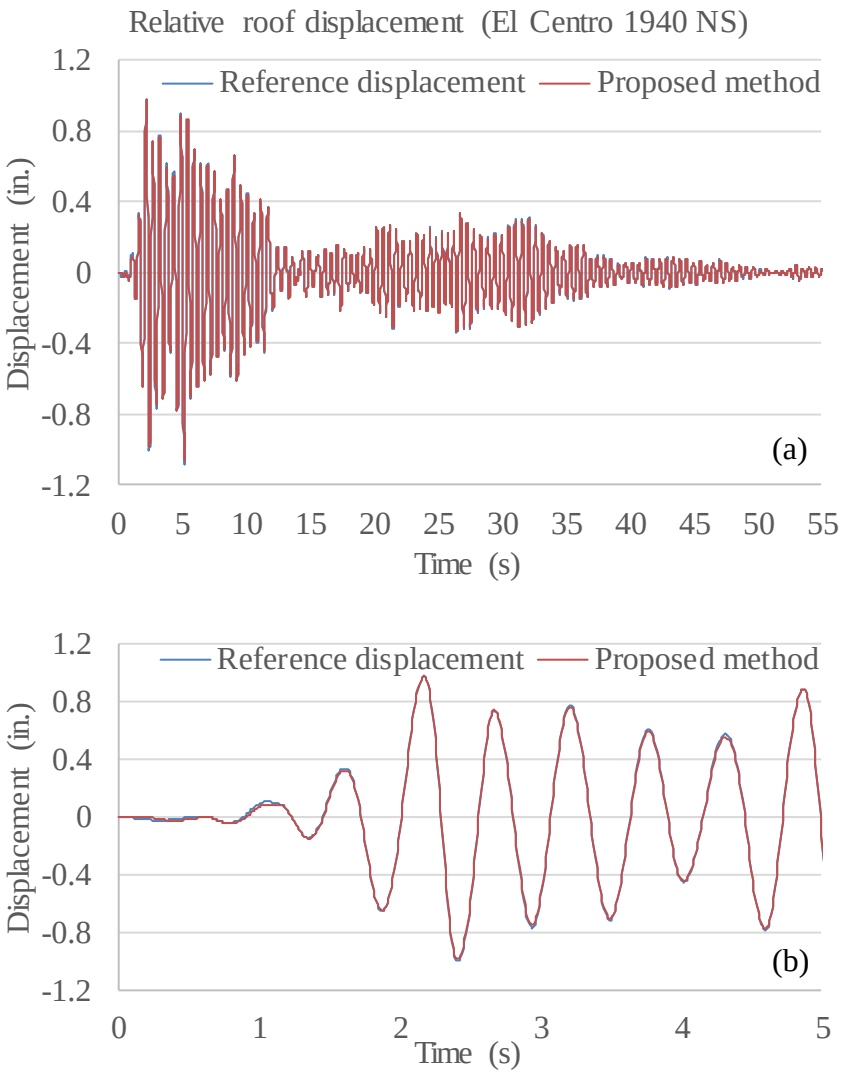

Figure 4-8: Relative roof displacement with zero-padding: (a) full record; (b) detailed comparison

The proposed method was also applied to another case study which involves the measured response of the Holiday-Inn building (Figure 4-9) during the 1994 Northridge earthquake. The records that were chosen for this study are the roof and the ground accelerations, channels 9 and 16, respectively, for both corrected and uncorrected (raw data) acceleration measurements. In both cases, using the corrected and raw acceleration measurements, the proposed method was able to reconstruct the relative displacement between the roof and the base with very high accuracy as

shown in Figure 4-10. Corrected displacement, which is available from the CESMD website and they derived it from the corrected acceleration measurements, for the same channels is provided from Center for Engineering Strong Motion Data (CESMD) [19].

Figure 4-9: Holiday-Inn building

The uncorrected acceleration measurements do not have a constant sampling time. However, since the difference between the time steps is very minimal it was assumed to be constant sampling time for calculating the relative displacement. As shown in Figure 4-10, there is no large difference between the obtained displacements from corrected or uncorrected measurements and the provided displacement from the Center for Engineering Strong Motion Data, which was also obtained from the roof and base acceleration measurements but with different approach.

The error between the estimated displacement and the reference displacement is estimated using the Frequency Domain Error (FDE) Index [17]. The FDE index is selected here due to its

effectiveness, especially in its ability to distinguish between the amplitude error and the phase error. The error from the FDE index is always between 0 and 1, where the 0 index means zero error and 1 means 100% error [17]. The amplitude difference between the estimated displacement from acceleration measurements and the processed displacement from CESMD is 1.6% based on the FDE index for the full length of the record.

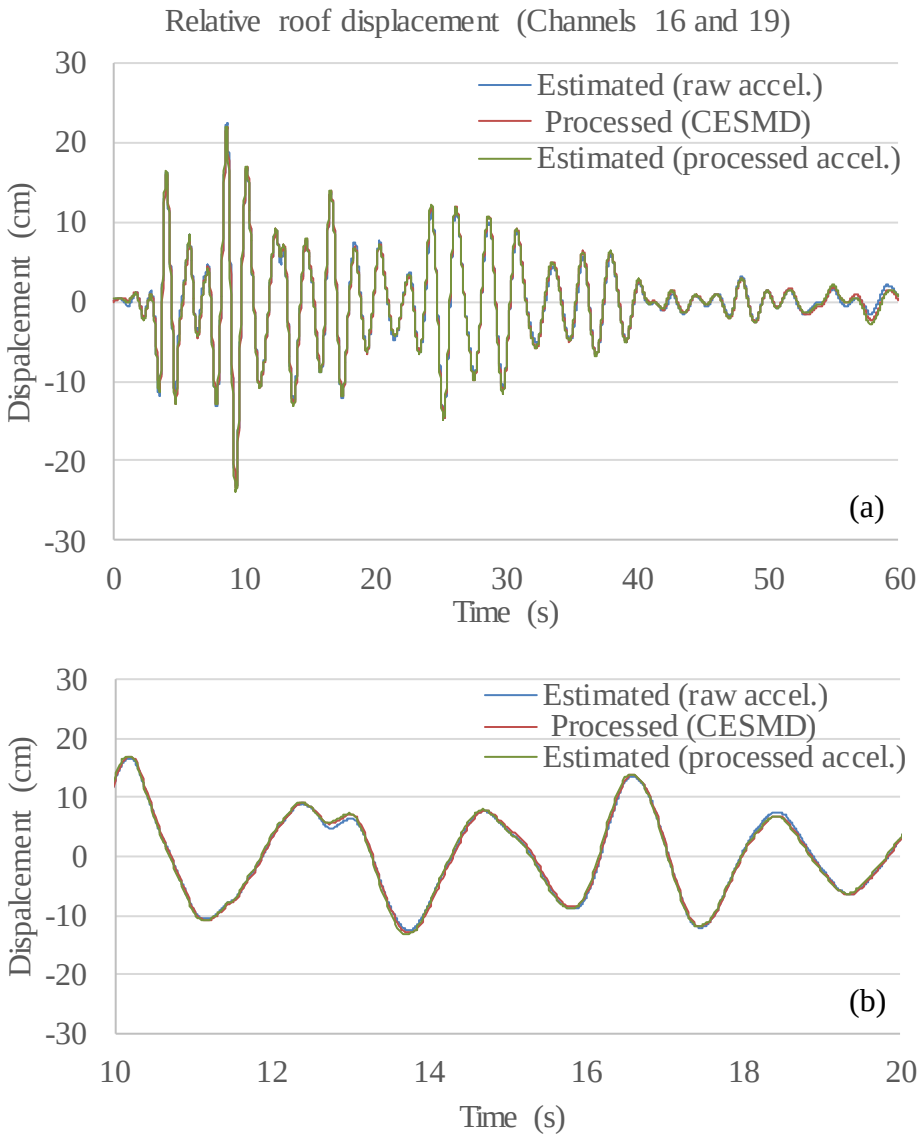

Figure 4-10: Holiday-Inn building, 1994 Northridge earthquake: (a) full record; (b) detailed comparison

4.2.4. Experimental results

The proposed method to estimate displacement in 4.2.3 is tested using the physical small-scale six-story structure. The small-scale six-story structure is subjected to different earthquake records using the shake table. In this experiment, eight accelerometers were used, one accelerometer at each level and two at the base (Figure 4-12). Acceleration measurements from the roof and the base accelerometers were used to estimate the relative roof displacement.

To have a reference measurement to compare with, an IOS application that was developed by Min et al. [20] was used. The real-time image-processing for non-contact monitoring (RINO) app was used to track the roof displacement. RINO app works by tracking a colored target (Figure 4-11), which is two circles with two different colors for each circle. RINO app tracks the position of the centroid of the two circles and provides the displacement of the center between these two circles. For this experiment, a colored target was attached to the small-scale six-story structure at the roof diaphragm to track the roof displacement (Figure 4-12). The RINO app was installed on an IPhone 6 which was fixed facing the colored target on a tripod. The accuracy of RINO had been verified by tracking the ground displacement and the shake table displacement, and both were compared with the embedded LVDT in the shake table, satisfactorily.

Figure 4-11: RINO colored target

Figure 4-12: Test setup and instrumentation

Even though RINO is adjusted to have a 60 Hz uniform output sampling rate, the output sampling rate is not fixed to 60Hz where few data are sampled at 30Hz or less, due to the limitation of the device such as the temporary memory limitation. To overcome the sampling rate issue in RINO, the output was interpolated to have a fixed 60Hz sampling rate using the time stamps from RINO. Uniform sampling rate is necessary for synchronizing the displacement from RINO with the displacement from the shake table.

The shake table has an embedded LVDT which measures the ground displacement, for this experiment the LVDT was set to have sampling rate of 125 Hz. The ground displacement signal was downsampled to 60Hz to be consistent with the displacement from RINO and obtain the relative roof displacement. Synchronization is critical and has direct impact on the produced

displacement. In order to synchronize the ground displacement measured by the shake table LVDT with the roof displacement recorded by RINO, a sine wave with a long period of eight seconds was added to the earthquake records after the free vibration of the structure died out (Figure 4-13). This sine wave synchronization method was tested on the numerical model to ensure the peak displacement of the ground and the roof displacements occur at the same time. The zero-crossing of the sine waves is a good point for synchronizing the roof and the ground displacements (Figure 4-13).

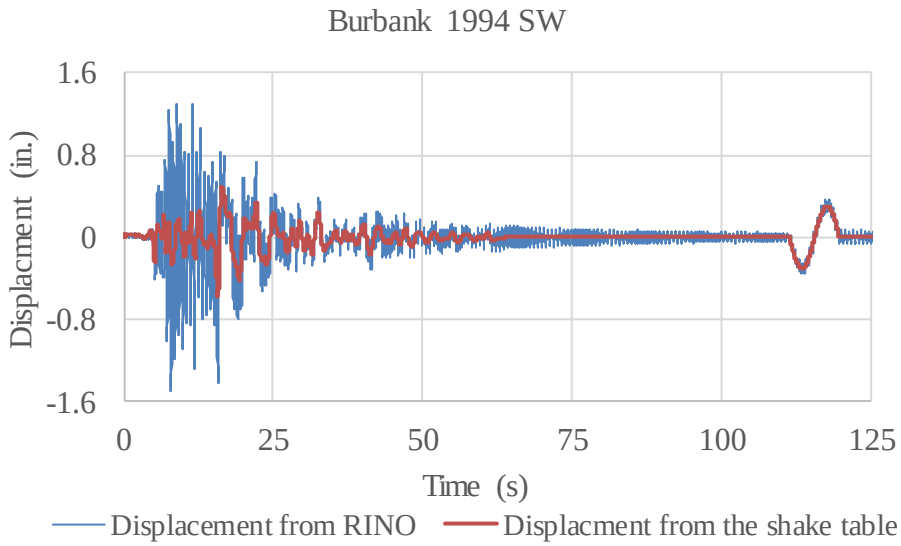

Figure 4-13: Synchronization of displacements measured from the shake table and RINO using the sine wave

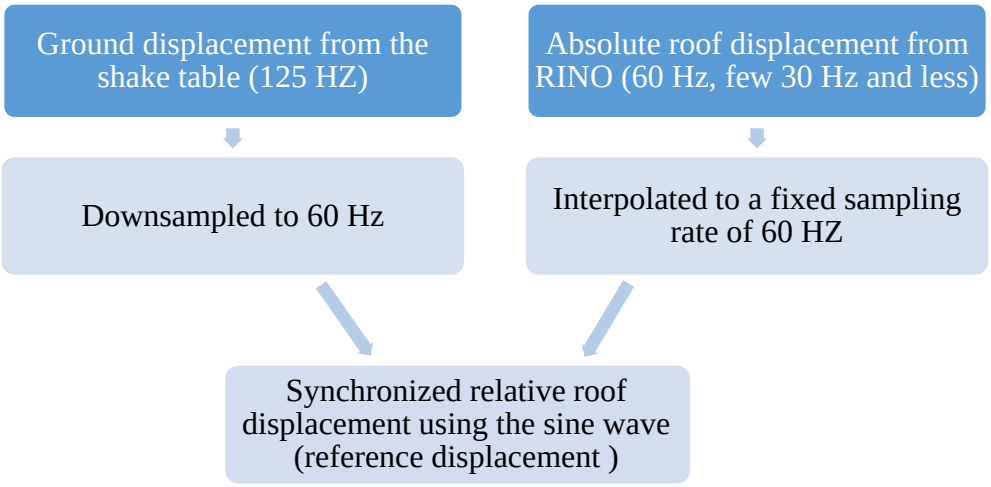

Figure 4-14: Procedures for obtaining the reference relative roof displacement

After obtaining the reference roof displacement, the next step is to estimate the relative displacement from acceleration measured at the ground and the roof. As shown in Figure 4-7, the window size has a direct impact on the accuracy of the estimated displacement. The results shown in Figure 4-7 were from numerical analysis; for the experimental results the same window size sensitivity test is performed and shown in Figure 4-15. The error level in the experimental sensitivity analysis is higher than the numerical analysis due to the measurement noise and other inherent errors. Both analyses have agreement in terms of the range of effective window size factor, which is between three to six times the fundamental period of the structure. It is recommended to try several window sizes, at least within the suggested range, to increase the accuracy of the estimated displacement.

The optimal window size factor for this experiment is 4.30 as shown in Figure 4-15 for Burbank 1994 SW and Wrightwood 1994 NS records. Optimal window size might differ based on

the fundamental period of the structure and the sampling rate. The optimal window size is selected based on the root-mean-square error and the peak error.

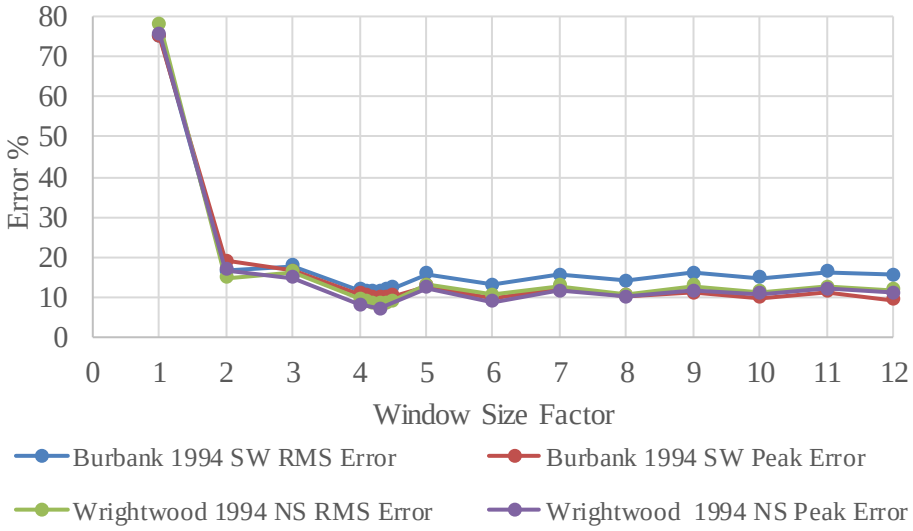

Figure 4-15: Window size factor sensitivity for experimental results

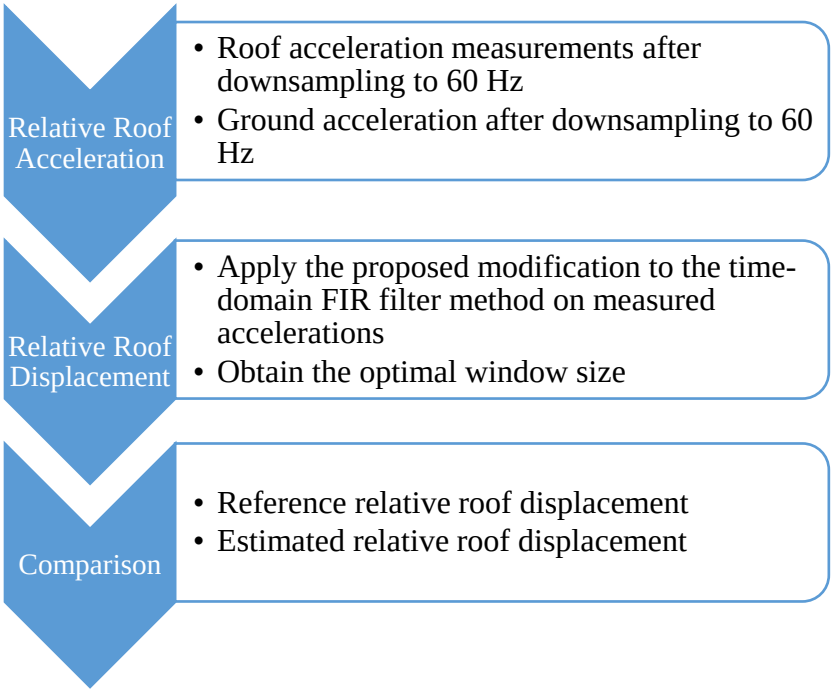

Figure 4-16: Procedures for roof displacement estimation and comparison with reference displacement

The first experiment uses the Wrightwood 1994 NS record (Figure 4-17) on the shake table with a peak acceleration of 22 in/s^2. This earthquake record was simulated using the shake table while the structure was attached, and then the structure acceleration responses were collected using the accelerometers as shown in Figure 4-12. Using the collected acceleration measurements, the roof displacement was estimated using the proposed method in 4.2.3. The estimated displacement is compared to the reference signal as shown in Figure 4-18. The reference relative roof displacement was measured using RINO and the embedded LVDT in the shake table following the procedures shown in Figure 4-14 and Figure 4-16.

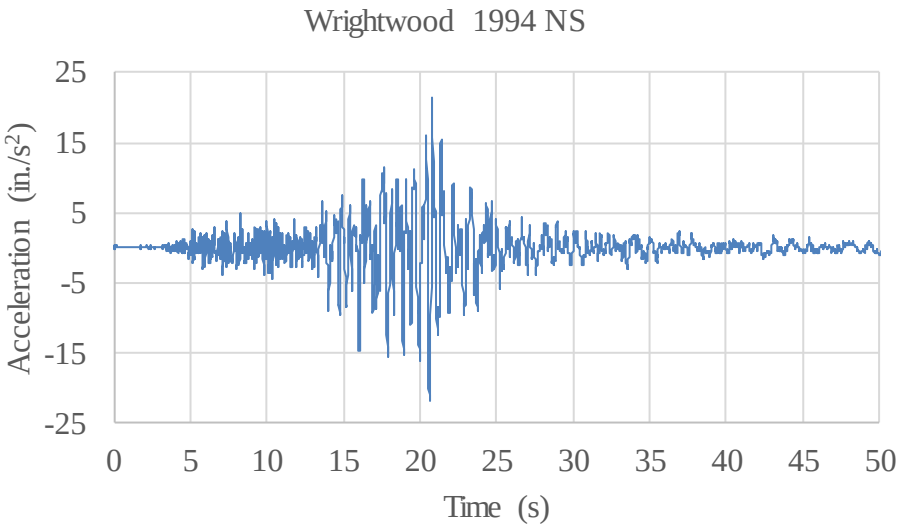

Figure 4-17: Ground acceleration for Wrightwood 1994 NS

The estimated displacement using the proposed enhancement to the time-domain FIR filter method described in 4.2.3 showed relatively accurate estimation when compared with the reference displacement. The FDE index for Wrightwood 1994 NS run was calculated to be 7.8% error in the amplitude and 2.4% in the phase error for the full-length record, and the peak error

was 7% for this case. The phase error is most likely introduced by the synchronization procedures. The amplitude error might be from resampling and filtering processes by the moving-time window.

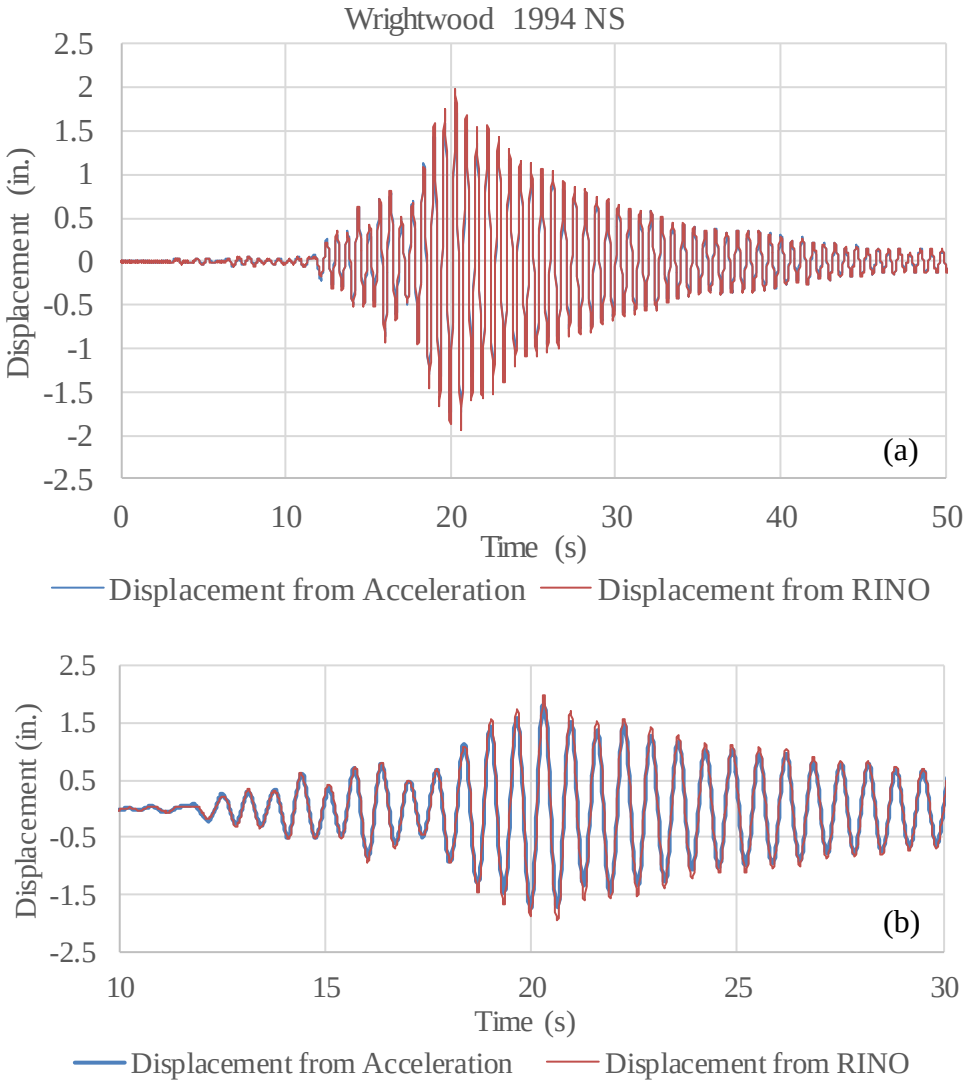

Figure 4-18: Relative roof displacement for Wrightwood 1994 NS: (a) full record; (b) detailed comparison

The second experiment is based on the Burbank 1994 SW record after scaling it down to 0.1g (Figure 4-19). This earthquake was simulated on the shake table and the acceleration measurements were collected by the attached accelerometers. The absolute roof displacement was

tracked using RINO. The procedures of obtaining the reference relative roof displacement was by following the same procedures discussed in Figure 4-14. The estimated displacement from acceleration was obtained by applying the proposed modification to the time-domain FIR filter method.

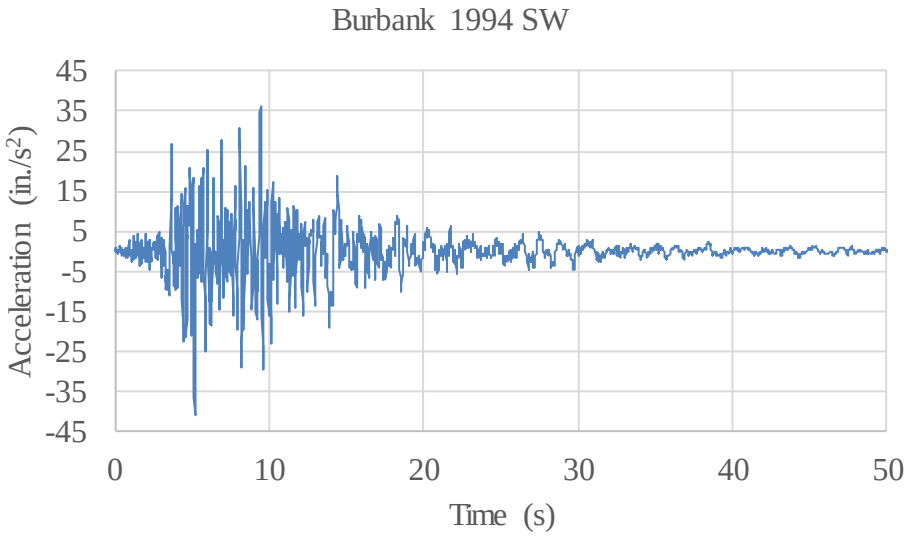

Figure 4-19: Ground acceleration for Burbank 1994 SW

The reference displacement and the estimated displacement are shown in Figure 4-20. The estimated relative roof displacement shows relatively good accuracy in comparison to the reference displacement. The FDE index [17] for this experiment was calculated to be a 10% difference in amplitude and 2.5% error in phase between the two records for the full-length record. The peak error is 9.7% for this case.

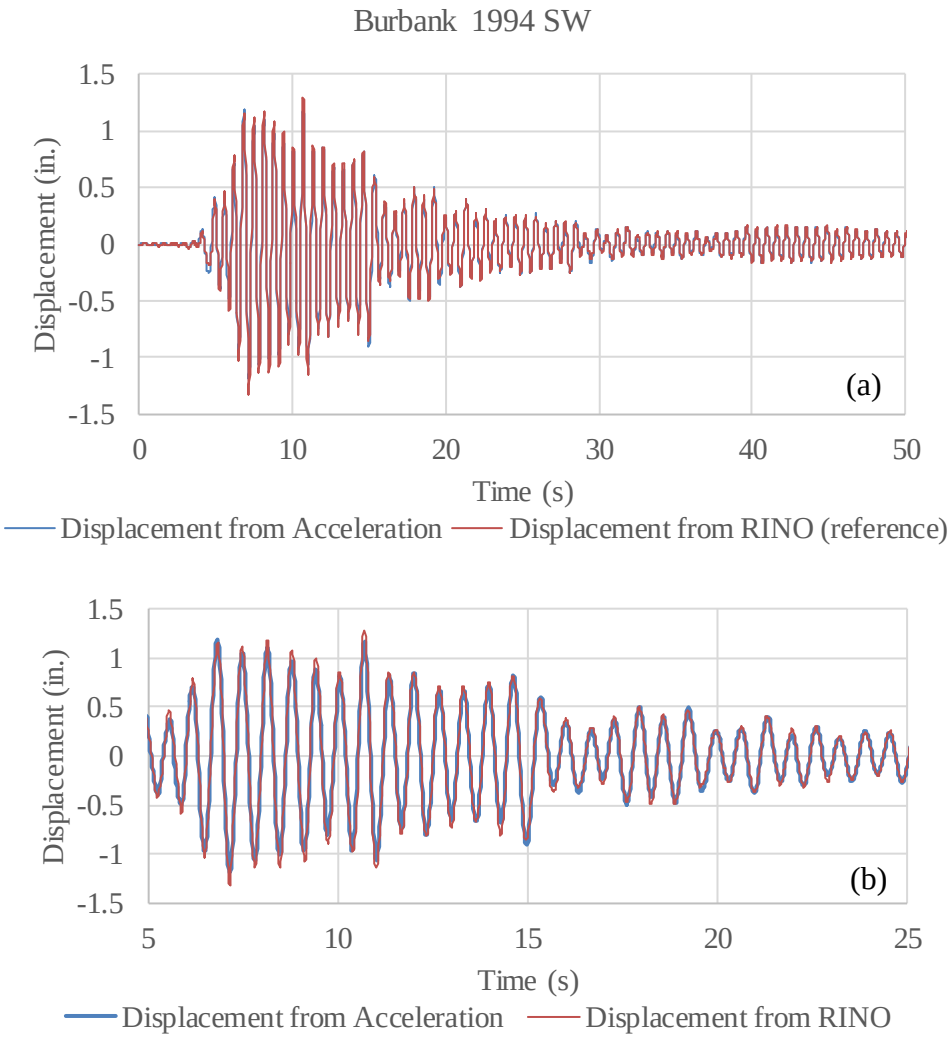

Figure 4-20: Relative roof displacement for Burbank 1994 SW: (a) full record; (b) detailed comparison

Based on the pervious numerical and experimental results, the proposed method can be used to obtain the displacement from acceleration measurements with relatively good accuracy. The window size is the key in estimating accurate displacement. Using inappropriate window size will lead to inaccurate displacement estimation with significantly high error.

4.3. Displacement Estimation Using Strain and Acceleration Measurements

4.3.1. Using strain measurements

Estimating displacement throughout strain measurements can be accomplished by using the linear relationship between displacement response and strain response. For a system that has a displacement response $\{u\}_{n\times1}$ and a strain response $\{\varepsilon\}_{m\times1}$, where n and m are the number of measured displacement and strain points, respectively [3], by using modal analysis and the modal coordinates q the displacement can be estimated as follows:

$$\{\varepsilon\}_{m\times1} = \Psi_{m\times r}\{q\}_{r\times1} \tag{4-7}$$

$$\{u\}_{n\times1} = \Phi_{n\times r}\{q\}_{r\times1} \tag{4-8}$$

By substituting equation (4-7) into equation (4-8), the displacement $\{u\}$ can be written as

$$\{u\}_{n\times1} = \Phi_{n\times r}\Psi^{+}_{r\times m}\{\varepsilon\}_{m\times1} \tag{4-9}$$

Where Φ and Ψ are the mass-normalized mode shapes of displacement and strain respectively, and the + represents pseudo inverse. In equation (4-9) displacement can be derived based on the strain measurements if the mass-normalized strain and displacement mode shapes are known [3]. Jong Park et al. [3] used this approach using a simply-supported beam with uniform mass across the beam section. Both displacement and strain mode shapes were mass-normalized in their study, which includes numerical and experimental results [3].

4.3.2. Proposed modification based on an α-factor method and modal participation mass ratios

The shown method in 4.3.1 is modified in this section to be applied to small-scale six-story structure. One of the main challenges is the need to obtain the mass-normalized mode shapes, which require at least one output to be measured at the same location of the input excitation in experimental modal analysis. Performing experimental modal analysis to building structures with measuring the output at the same location of the input is difficult and costly. The proposed method can estimate the displacement of building structures without the need to know the mass-normalized mode shapes. Two additional factors are added to equation (4-9) as shown in equation (4-10)

$$\{u\}_{n\times 1} = \alpha(\Gamma_{n\times n}\Phi_{n\times r}\Psi^{+}_{r\times m}\{\varepsilon\}_{m\times 1}) \tag{4-10}$$

Where α is a correction factor that can be calculated based on equation (4-11) [3]. Γ is the modal participation mass ratios matrix that will be discussed at the end of this section. Φ and Ψ are the displacement and strain mode shapes, respectively. For both displacement and strain mode shapes, the maximum value of each mode shape vector is normalized to 1. $S_{d,acc}$ is the power spectral density (PSD) of the displacement estimated using acceleration measurements, $S_{d,strain}$ is the PSD from the estimated displacement using strain measurements. f_n is the identified fundamental period of the structure from the PSD

$$\alpha = \frac{\sqrt{S_{d,acc}(f_n)}}{\sqrt{S_{d,strain}(f_n)}} \tag{4-11}$$

modal participation mass ratios can be calculated through generalized mass matrix M and the displacement mode shapes [21] as shown in the following equations:

$$\widehat{m} = \phi^T M \phi \tag{4-12}$$

$$\bar{L} = \phi^T M \bar{r} \tag{4-13}$$

$$\Gamma = \frac{\bar{L}}{\widehat{m}} \tag{4-14}$$

Where $\bar{r}$ is an influence vector that represents displacements of the masses if a unit ground displacement was applied statically [21].

Mass matrix might be estimated based on the structure geometry and known material properties or by performing experimental modal analysis [4]. By assuming the building structures have uniform mass distribution, another suggested simpler approach to estimate modal participation mass ratios is to assume a diagonal lumped mass matrix $M_{n\times n}$ with a value equal to one, where n is the number of modes to be considered. For the numerical model in chapter 3 the mass matrix was taken as shown in equation (4-15)

$$M = \begin{bmatrix} 1 & 0 & 0 & 0 & 0 & 0 \\ 0 & 1 & 0 & 0 & 0 & 0 \\ 0 & 0 & 1 & 0 & 0 & 0 \\ 0 & 0 & 0 & 1 & 0 & 0 \\ 0 & 0 & 0 & 0 & 1 & 0 \\ 0 & 0 & 0 & 0 & 0 & 1 \end{bmatrix} \tag{4-15}$$

Using the assumed mass matrix in equation (4-15) the modal participation mass ratios Γ can be estimated with relatively high accuracy as shown in Table 4-2.

Table 4-2: Modal participation mass ratios

Mode order	Modal participation mass ratios	
	From SAP2000	From the assumed mass matrix
Mode 1	0.8649	0.8766
Mode 2	0.0896	0.0801
Mode 3	0.0270	0.0305
Mode 4	0.0100	0.0080
Mode 5	0.0034	0.0042
Mode 6	0.0007	0.0005

Modal participation mass ratios in Table 4-2 were obtained from SAP2000 and from the assumed mass matrix using equation (4-14) . Through comparison, we can see that the assumed mass matrix can be used to calculate the modal participation mass ratios with a high accuracy in comparison with using the actual mass matrix.

The proposed α-factor method and modal participation mass ratios to estimate displacement from strain in equation (4-10) was applied using the full numerical model introduced in chapter 3. Two virtual strain gauges are simulated at each end of each column in the full numerical model, with a total of twelve virtual strain gauges for the whole structure. The first numerical test was conducted by applying the Burbank 1994 SW as the input ground motion in the numerical model, then the acceleration and strain measurements were obtained from the numerical model in SAP2000. The relative roof displacement of the numerical model was obtained using the α-factor method as shown in Figure 4-21. From these numerical results we can conclude that the proposed method can effectively estimate the structural displacement from strain measurements. The amplitude error of the estimated displacement using the proposed method for this numerical case is 1.9% based on the FDE index (Table 4-3).

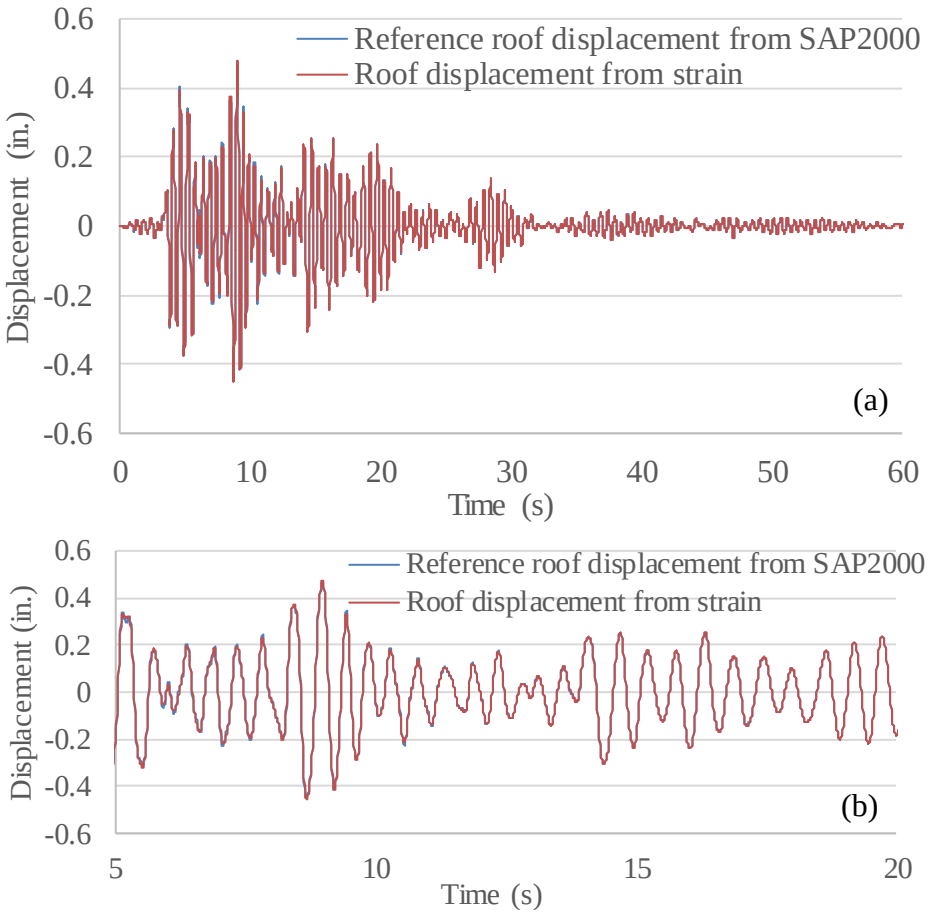

Figure 4-21: Estimated displacement from strain for Burbank 1994 SW: (a) full record; (b) detailed comparison

Another numerical case study was conducted by using the El Centro 1940 NS (Figure 4-4) as the input ground motion in the numerical model, and the relative roof displacement of the numerical model was then obtained from strain measurements as shown in Figure 4-22. For this numerical case the proposed α-factor method was able to convert the strain measurement to relative displacement with a high accuracy based on the shown numerical results. The amplitude error of the estimated displacement using the proposed method for the El Centro 1940 NS earthquake record is 1.3% based on the FDE index (Table 4-3).

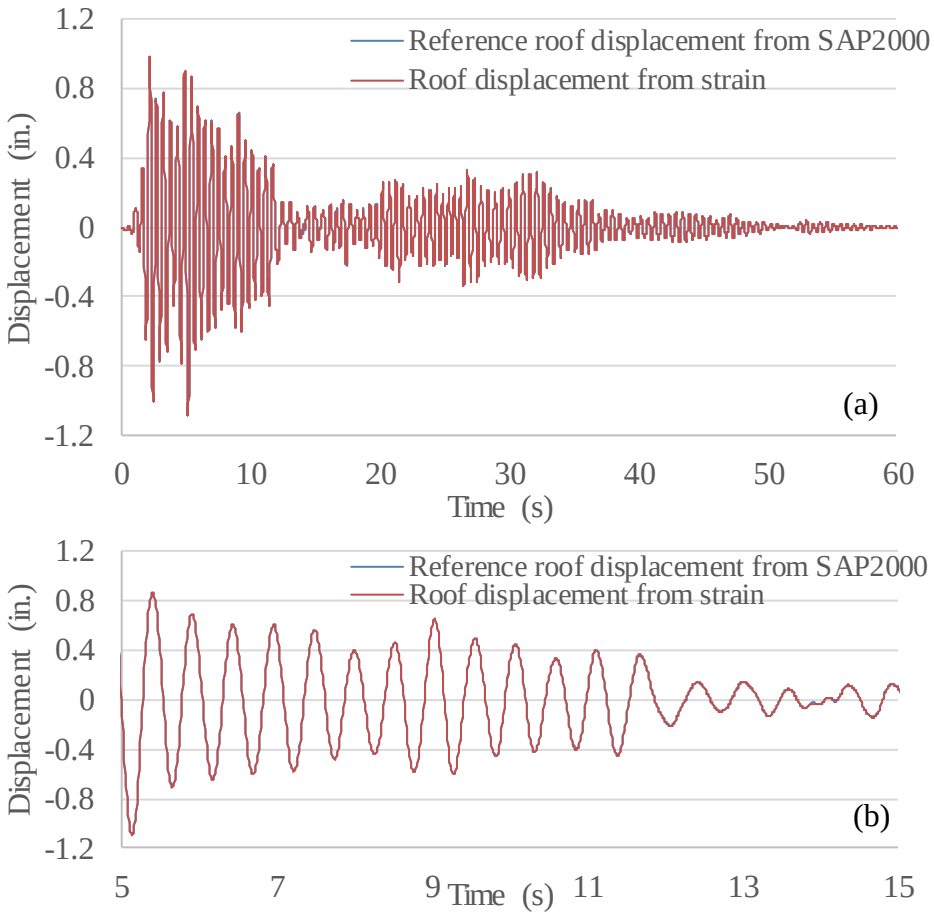

Figure 4-22: Estimated displacement from strain for El Centro 1940 NS: (a) full record; (b) detailed comparison

Estimating displacement through strain measurements using the proposed α-factor method and modal participation mass ratios from the assumed mass matrix was able to produce accurate results. The key feature in this proposed method is that it does not require mass-normalized mode shapes.

4.4. Data Fusion

Displacement estimation using data fusion by combining acceleration and strain measurements can offer more realistic output than using a single type of measurement. For example, in bridges where the pseudo-static displacement can be significant or for high-rise buildings under high wind load, estimating displacement through acceleration measurements and the following signal processes will neglect the pseudo-static displacement. Combining strain and acceleration measurements will reserve the pseudo-static displacement. Equation (4-3) can be expanded as shown in (4-16) to include strain measurements.

$$\underset{u}{\text{Min}}\,\Pi = \frac{1}{2}\left\| L_a\left(L_c u_i - \Delta t^2 \bar{a}_i\right)\right\|_2^2 + \frac{\lambda^2}{2}\left\| u_i - D_i\{\varepsilon\}\right\|_2^2 \tag{4-16}$$

The solution of Equation (4-16) is shown in Equation (4-17)

$$u_i = \left(L^T L + \lambda^2 I\right)^{-1}\left(L^T L_a \bar{a}_i \Delta t^2 + \lambda^2 D_i\{\varepsilon\}\right) \tag{4-17}$$

$$D\{\varepsilon\} = \alpha(\Gamma_{n\times n}\widehat{\Phi}_{n\times r}\widehat{\Psi}^{+}_{r\times m}\{\varepsilon\}_{m\times 1}) \tag{4-18}$$

Thus the shown equation (4-17) is expressed in both strain and acceleration measurements [3].

The same numerical cases that were discussed in section 4.2.3 are shown here but with the data fusion method applied, which combines acceleration and strain measurements and applies an overlapping time window. In Figure 4-23 the relative roof displacement was obtained from data fusion using El Centro 1940 NS as input ground motion in the numerical model. The numerical results indicate that the relative displacement can be obtained using the data fusion method. The displacement can be estimated by combining the acceleration and strain measurements for building structures without the need for the mass-normalized mode shapes. The amplitude error of the

estimated displacement using the proposed data fusion method for this numerical case is 1% based on the FDE index (Table 4-3).

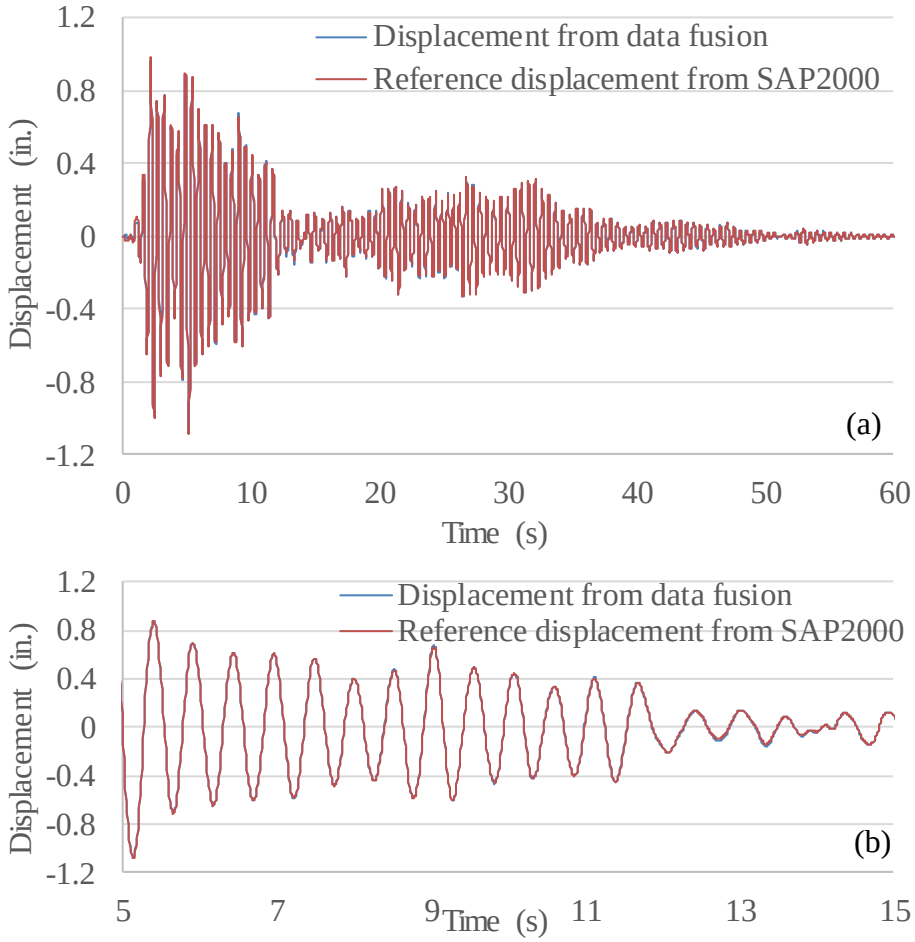

Figure 4-23: Estimated displacement from data fusion for El Centro 1940 NS: (a) full record; (b) detailed comparison

The second numerical case is using Burbank 1994 SW as an input excitation in the numerical model. The relative roof displacement was estimated using the data fusion method. The estimated displacement for this case has a good accuracy as shown in Figure 4-24. The amplitude error of the estimated displacement using the proposed data fusion method for this numerical case is 1.1 % based on the FDE index (Table 4-3).

Table 4-3: Error in the estimated displacement from strain measurements

	FDE index, %	
	El Centro 1940 NS	Burbank 1994 SW
The α-factor method	1.3	1.9
Data fusion method	1	1.1

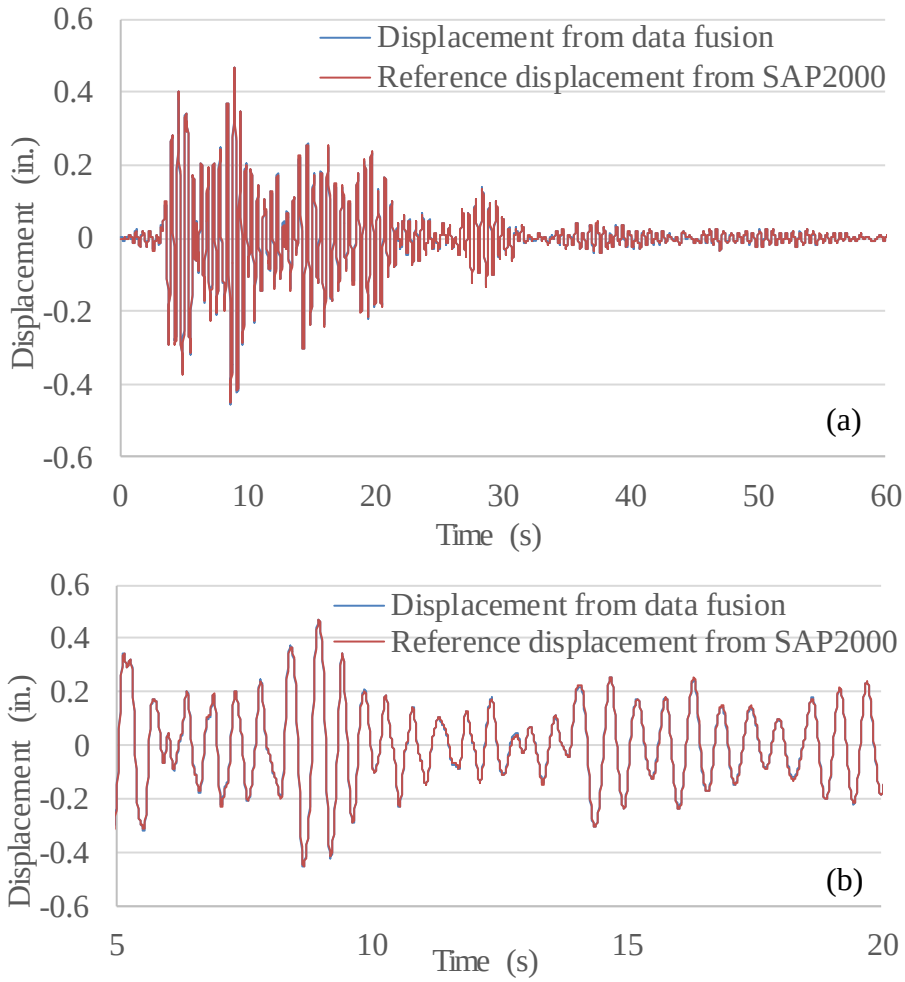

Figure 4-24: Estimated displacement from data fusion for Burbank 1994 SW: (a) full record; (b) detailed comparison

4.5. Summary

In this chapter, different methods were discussed to estimate structural displacement by using acceleration measurements alone or by combining acceleration with strain measurements. Three methods were shown. In the first method, the proposed modification to the time-domain FIR filter method using the zero padding technique to recover the missing parts, at the beginning and at the end of the displacement record, in the original time-domain FIR filter method [2]. The numerical investigation and experimental results shows that proposed modification to the time-domain FIR filter method can be used to estimate the structural displacement from acceleration measurements with a high accuracy if the window size is selected properly.

The second proposed method is the proposed α-factor method and the modal participation mass ratios, which estimated from the assumed mass matrix. This method estimate displacement from strain measurements for building structures without the need for the mass-normalized mode shapes. Calculating the modal participation mass ratios was discussed by using the actual mass matrix or by using the assumed mass matrix. The last method is the data fusion method which is a combination of the first and the second methods, where data fusion method uses both acceleration and strain measurements with an overlapping moving time window to estimate displacement. The numerical results showed that estimating displacement from acceleration and strain measurements is possible for building structures without the need to know the mass-normalized mode shapes.

The proposed α-factor method is based on strain measurements and a scaling factor from acceleration measurements. On the other hand, the data fusion method estimate the displacement from acceleration and strain measurements and applies the proposed modified overlapping moving time window with the zero padding technique.

CHAPTER 5: CONCLUSIONS AND FUTURE WORK

5.1. Conclusions

Different methods to estimate structural displacement using acceleration and strain measurements were presented in this study. The first method is based on the proposed modification to the time-domain FIR filter method to estimate the displacement using acceleration measurements. The second method, the α-factor method, combines the modal participation mass ratios, with a scaling factor derived using displacement obtained from acceleration measurements. A third method was presented for estimating structural displacement through the combined use of acceleration and strain measurements.

The first chapter provides a general description of problems related to the estimation of structural displacement based on the use of acceleration and strain measurements. Emphasis was placed on the challenges in using indirect measurements to estimate displacement. An example of such challenges is the unrealistic drift that appears in the estimated displacement from acceleration. Furthermore, the challenge of estimating displacements from strain involves the need for mass-normalized mode shapes. A detailed discussion about these challenges and its sources are presented in chapter 2.

The second chapter includes a literature review of previous studies and related research for estimating displacement from acceleration and strain measurements. Extensive discussion is presented about the sources and solutions of some known challenges in using acceleration measurements to estimate displacements of structures. Main focus was placed on the suspected sources causing the unrealistic drift that appears in the double-integrated acceleration. Common correction methods to solve this anomaly were also described.

The third chapter presents the details of designing and constructing a small-scale six-story structure for use in experiments. In addition, details of numerical modeling of the small-scale six-story structure in SAP2000 are described. Two numerical models were developed in SAP2000, one represents the full structural components and the other is a simplified (reduced) numerical model. This chapter also describes the procedures used in the system identification tests and the subsequent identified dynamic properties of the small-scale six-story structure. The numerical models were calibrated using the data obtained from system identification. The small-scale structure and the two numerical models were used in the numerical investigation and experimental validation of the proposed methods in chapter 4.

The fourth chapter addresses the challenges identified in the first and second chapters for the three proposed methods of estimating displacement. The first method is based on modifying the time-domain FIR filter method to avoid the missing parts of the reconstructed displacement based on the original method. The numerical and experimental results showed relatively high accuracy of the modified method for displacement estimation using acceleration measurements. The window size is the key factor that directly affects the accuracy of the estimated displacement signal. Amplitude error is directly related to the moving window size; the optimal window depends on the fundamental frequency of the structure and the sampling rate of the output signals. This chapter also presents a sensitivity study to identify the optimal window size.

The second proposed method for estimating structural displacement is based on the use of strain measurements without need for mass-normalized mode shapes. This method allows the uses of arbitrarily normalized displacement and strain mode shapes to estimate the displacement from strain, and the modal participation mass ratios are used to calibrate the contribution of each mode. An assumed diagonal mass matrix is used to obtain the modal participation mass ratios. The results

showed that the assumed mass matrix produced very close ratios in comparison to the ratios obtained from SAP2000, and the estimated displacements from strain measurements showed great accuracy using the proposed strategy.

The data fusion method was also discussed in chapter 4. This method combines acceleration and strain measurements to estimate structural displacement under the framework of the modified time-domain FIR filter method. The data fusion. The data fusion method applies the moving time window with the proposed zero-padding technique to estimate displacement from acceleration. The method uses the α-factor to estimate displacement from strain measurements.

In summary, several challenges in using indirect measurements to estimate displacements of structures were explored. Major finding in this study include the effective use of zero-padding technique to recover the missing parts, at the beginning and end, of the estimated displacement (from acceleration) in the original time-domain FIR filter method. The proposed α-factor method eliminates the need for mass-normalized mode shapes to estimate displacement from strain measurements.

5.2. Future Work

Future research should be focused on experimental validation of the proposed α-factor and data fusion methods for linear structural response. Strain gauges will be installed to measure strain at the columns of the small-scale and full-scale structures, in addition to acceleration and displacements measured at each floor.

Filtering and other signal processing involved in the estimation of displacement using acceleration measurements lead to removal of the pseudo-static component in the estimated

displacement. The pseudo-static displacement might be significant in evaluating the damage state of structures. One example of structural response that contains pseudo-static displacement is the response of high-rise building structures subjected to wind load. By using acceleration only to estimate such displacements, the pseudo-static components may get lost. The effectiveness of using strain measurements in preserving both the pseudo-static and permanent displacements needs to be evaluated.

REFERENCES

1. Skolnik, D.A. and J.W., Wallace, *Critical Assessment of Interstory Drift Measurements.* Journal of Structural Engineering, 2010. **136**(12): p. 1574-1584.

2. Lee, H.S., Y.H. Hong, and H.W. Park, *Design of an FIR filter for the displacement reconstruction using measured acceleration in low-frequency dominant structures.* International Journal for Numerical Methods in Engineering, 2010. **82**(4): p. 403-434.

3. Park, J.W., S.H. Sim, and H.J. Jung, *Displacement Estimation Using Multimetric Data Fusion.* IEEE/ASME Transactions on Mechatronics, 2013. **18**(6): p. 1675-1682.

4. Cornwell, P., S.W. Doebling, and C.R. Farrar, *Application of the strain energy damage detection method to plate-like structures.* Journal of Sound and Vibration, 1999. **224**(2): p. 359-374.

5. Housner, G.W., *Ground displacement computed from strong-motion accelerograms.* Bulletin of the Seismological Society of America, 1947. **37**(4): p. 299-305.

6. Iwan, W.D., M.A. Moser, and C.-Y. Peng, *Some observations on strong-motion earthquake measurement using a digital accelerograph.* Bulletin of the Seismological Society of America, 1985. **75**(5): p. 1225-1246.

7. Yang, J., J.B. Li, and G. Lin, *A simple approach to integration of acceleration data for dynamic soil–structure interaction analysis.* Soil Dynamics and Earthquake Engineering, 2006. **26**(8): p. 725-734.

8. Djurić, *Z., Mechanisms of noise sources in microelectromechanical systems.* Microelectronics and Reliability, 2000. **40**(6): p. 919-932.

9. Boore, D.M., *Analog-to-digital conversion as a source of drifts in displacements derived from digital recordings of ground acceleration.* Bulletin of the Seismological Society of America, 2003. **93**(5): p. 2017-2024.

10. Berg, G.V., and G.W., Housner, *"Integrated velocity and displacement of strong earthquake ground motion."* Bulletin of the Seismological Society of America 51.2 (1961): 175-189.

11. Trifunac, M.D. *Zero baseline correction of strong-motion accelerograms.* Bulletin of the Seismological Society of America, 1971. **61**(5): p. 1201-1211.

12. Boore, D.M., *Effect of baseline corrections on displacements and response spectra for several recordings of the 1999 Chi-Chi, Taiwan, Earthquake.* Bulletin of the Seismological Society of America, 2001. **91**(5): p. 1199-1211.

13. Foss, G. and E. Haugse. *Using modal test results to develop strain to displacement transformations*. Proceedings of the 13th International Modal Analysis Conference. 1995.

14. Pisoni, A. C., C., Santolini, D. E., Hauf, and S., Dubowsky. *Displacements in a vibrating body by strain gage measurements.* Proceedings of the 13th International Society for Optical Engineering, 1995.

15. Kang, L. H., D. K., Kim, and J. H., Han. E*stimation of dynamic structural displacements using fiber Bragg grating strain sensors*. Journal of sound and vibration, 305(3), 534-542, 2007.

16. Wang, Z. C., D., Geng, W. X., Ren, and H. T., Liu. *Strain modes based dynamic displacement estimation of beam structures with strain sensors.* Smart Materials and Structures, 2014. *23*(12): p. 1-9.

17. Dragovich, J.J. and A. Lepage. *FDE index for goodness-of-fit between measured and calculated response signals.* Earthquake Engineering and Structural Dynamics, 2009. **38**(15): p. 1751-1758.

18. Gavin, H.P., R. Morales, and K. Reilly, *Drift-free integrators.* Review of Scientific Instruments, 1998. **69**(5): p. 2171-2175.

19. Center for Engineering Strong Motion Data (CESMD). (2017). http://www.strongmotioncenter.org, last accessed November, 2016.

20. Min, J. H., N. J., Gelo, and H., Jo, (2015). *Non-contact and Real-time Dynamic Displacement Monitoring using Smartphone Technologies*. Journal of Life Cycle Reliability and Safety Engineering, 4(2), 40-51.

21. Irvine, T., *Effective modal mass and modal participation factors.* http://www.vibrationdata.com/tutorials2/ModalMass.pdf., last accessed December, 2016.